

Majoron-Driven Leptogenesis in Gauged $U(1)_{L_\mu-L_\tau}$ Model

Juntaro Wada^a *

^a*Department of Physics, University of Tokyo, Bunkyo-ku, Tokyo 113-0033, Japan,*

Abstract

We propose a novel leptogenesis scenario in the gauged $U(1)_{L_\mu-L_\tau}$ model. Achieving successful leptogenesis in the $U(1)_{L_\mu-L_\tau}$ symmetric phase is challenging due to the absence of a CP phase, caused by restriction from the gauge symmetry. To overcome this issue, we introduce an additional global symmetry, $U(1)_{B-L}$, and a scalar field Φ responsible for breaking this symmetry. Through the kinetic misalignment mechanism, the majoron field associated with $U(1)_{B-L}$ symmetry breaking has a kinetic motion in the early universe. Subsequently, time-dependent majoron field background induces the background CP phase dynamically, leading to successful leptogenesis in the $U(1)_{L_\mu-L_\tau}$ symmetric phase. Furthermore, majoron itself serves as a dark matter candidate in this scenario. As one of the phenomenological applications, we consider the model that can also explain the muon $g-2$ anomaly.

*wada@hep-th.phys.s.u-tokyo.ac.jp

1 Introduction

The origin of baryon asymmetry, or matter-antimatter asymmetry, in the current universe, remains a profound puzzle in particle physics and cosmology. Leptogenesis [1] stands out as a compelling mechanism capable of explaining the observed baryon asymmetry. In this mechanism, right-handed Majorana neutrinos play an important role; their mass breaks the lepton number and causes baryon number breaking through the sphaleron process [2], and their decay to the standard model leptons satisfies the conditions of CP violation and departure from thermal equilibrium, known as Sakharov’s conditions [3]. Furthermore, the seesaw mechanism [4–7] allows us to address the puzzle of the smallness of neutrino masses [8].

In this paper, our focus is on a model featuring the gauged $U(1)_{L_\mu-L_\tau}$ symmetry [9–12]. Within this framework, μ flavor particles carry +1 charge, while τ flavor particles carry -1 charge. This symmetry strongly influences the neutrino mass structure, because the second and third flavor leptons are charged under this symmetry whereas the first flavor is not. Consequently, the Dirac mass matrix exhibits a simple diagonal structure, and only specific components of the Majorana mass matrix are non-zero. To enable neutrino oscillation, we need to introduce scalars that break this gauged $U(1)_{L_\mu-L_\tau}$ symmetry [13, 14]. After $U(1)_{L_\mu-L_\tau}$ symmetry breaking, it remains non-trivial whether the observed neutrino oscillation parameters can be reproduced. In the minimal setup consistent with neutrino oscillations, several predictions for neutrino oscillation data have been obtained [15–20].

While the scale of $U(1)_{L_\mu-L_\tau}$ symmetry breaking does not significantly impact the consistency with neutrino oscillation data, it holds significance for other phenomena. A high breaking scale is favored in successful leptogenesis [21, 22], while a low breaking scale is motivated by contexts such as muon $g - 2$ anomaly [23–27], Hubble tension [28, 29], and searches for dark sector particles [30, 31].¹ Some efforts have been made to achieve successful leptogenesis with a low-scale $U(1)_{L_\mu-L_\tau}$ breaking scalar [37, 38]. However, these models lose predictive power for neutrino oscillation due to the need for more additional scalars that break $U(1)_{L_\mu-L_\tau}$ symmetry. The reason why we need more $U(1)_{L_\mu-L_\tau}$ breaking scalar is that firstly, the production of sufficient baryon asymmetry typically requires a high temperature which is far from the low $U(1)_{L_\mu-L_\tau}$ breaking scale. Then, at such high temperatures, the $U(1)_{L_\mu-L_\tau}$ symmetry can be restored, potentially leading to a lack of CP phases during leptogenesis due to symmetry restrictions. To circumvent this issue, additional scalars that break $U(1)_{L_\mu-L_\tau}$ symmetry and their interactions are necessary, compromising predictive power.

In our work, we propose a novel model capable of achieving successful leptogenesis with a low-scale $U(1)_{L_\mu-L_\tau}$ breaking without sacrificing predictive power for neutrino oscillation data. We introduce an additional symmetry, a global $U(1)_{B-L}$, and a scalar field Φ responsible for breaking this global symmetry. Suppose this scalar field Φ has a kinetic motion to the phase direction in the early universe, similar to the Affleck-Dine mechanism [39, 40]. Then a time-dependent background phase is induced, enabling successful leptogenesis in the $U(1)_{L_\mu-L_\tau}$ symmetric phase. This scenario can be realized through the kinetic misalignment mechanism [41–43], and the angular component of the

¹One can introduce the $U(1)_{L_\mu-L_\tau}$ charged dark matter candidate [32–36], but we will not discuss this possibility.

rotating field, majoron, can serve as a dark matter candidate. While leptogenesis with time-dependent background phase has been studied in several works [44–52], we incorporate the phenomenological aspects specific to the gauged $U(1)_{L_\mu-L_\tau}$ model. As one of the phenomenological applications, we demonstrate that our proposed scenario is applicable in models explaining the muon $g - 2$ anomaly.

The paper is organized as follows. In Sec. 2, we present our model and its basic properties, highlighting the challenges for successful leptogenesis in the $U(1)_{L_\mu-L_\tau}$ symmetric phase. In Sec. 3, we briefly explain how to achieve successful leptogenesis in the $U(1)_{L_\mu-L_\tau}$ symmetric phase. We then evaluate the produced baryon asymmetry and dark matter abundance, discussing various constraints on our model. In Sec. 4, we present the parameter space compatible with the observed baryon asymmetry and the dark matter abundance.

2 Model

Our model is constructed upon the framework of the gauged $U(1)_{L_\mu-L_\tau}$ symmetry [9–12]. In this framework, we assign charges to the $+1$ for μ flavor fields and -1 for τ flavor fields. To reproduce the neutrino mixing and be consistent with the neutrino oscillation data, we introduce three heavy right-handed neutrinos (denoted as N_e, N_μ , and N_τ) along with the standard model gauge singlet scalars, σ_μ and σ_τ .² They carry the $U(1)_{L_\mu-L_\tau}$ charges $0, +1, -1$, and $+1, -1$ respectively. Our model also contains $U(1)_{L_\mu-L_\tau}$ gauge boson Z' .

Furthermore, our model incorporates an additional symmetry, namely *global* $U(1)_{B-L}$, and a scalar field Φ responsible for breaking this global symmetry. Under this symmetry, we assign charges to the -1 for left-handed $SU(2)$ lepton doublets (ℓ_e, ℓ_μ , and ℓ_τ), the right-handed charged leptons (e_R, μ_R , and τ_R) and three heavy right-handed neutrinos (N_e, N_μ , and N_τ), while left-handed $SU(2)$ quark doublets Q and right-handed charged quarks u_R, d_R carry a $U(1)_{B-L}$ charge of $+1/3$. The singlet scalars, σ_μ, σ_τ and Φ , have $U(1)_{B-L}$ charge of -2 .

We summarise these charges assignments of the field content in Table 1.

Charges and Field Content							
	ℓ_e, e_R, N_e	ℓ_μ, μ_R, N_μ	$\ell_\tau, \tau_R, N_\tau$	σ_μ, σ_τ	Φ	Q, u_R, d_R	Others
$L_\mu - L_\tau$	0	+1	-1	+1, -1	0	0	0
$B - L$	-1	-1	-1	-2	-2	+1/3	0

Table 1: Assigned charges of the field content in our model.

²In our model, two scalar fields, σ_μ and σ_τ , are introduced to break the $U(1)_{L_\mu-L_\tau}$ symmetry. Alternatively, a model consistent with neutrino oscillations can be constructed using a single scalar field σ [18–20, 53–55]. However, in this case, the interaction involving σ^* , which is necessary to reproduce the correct neutrino mixing, explicitly breaks $U(1)_{B-L}$ and typically leads to a large majoron mass. Such a heavy majoron would spoil our scenario due to the overabundance of majoron dark matter.

Under this setup, we can write down the Lagrangian for the neutrino sector as follows:³

$$\begin{aligned} \mathcal{L}_N = & -\lambda_e N_e^c (\ell_e \cdot H) - \lambda_\mu N_\mu^c (\ell_\mu \cdot H) - \lambda_\tau N_\tau^c (\ell_\tau \cdot H) \\ & - \frac{1}{2} \lambda_{ee} \Phi N_e^c N_e^c - \lambda_{\mu\tau} \Phi N_\mu^c N_\tau^c - \lambda_{e\mu} \sigma_\mu N_e^c N_\mu^c - \lambda_{e\tau} \sigma_\tau N_e^c N_\tau^c + \text{h.c.} , \end{aligned} \quad (1)$$

where H is the Standard Model Higgs boson, and the dots indicate the contraction of the SU(2) indices between the lepton doublets and the Higgs doublet.

After the Higgs field H , and singlets σ_μ , σ_τ and Φ get their vacuum expectation value (VEVs),⁴ denoted as $\langle H \rangle = v/\sqrt{2}$, $\langle \sigma_\mu \rangle$, $\langle \sigma_\tau \rangle$ and $\langle \Phi \rangle$, these interaction terms lead to the neutrino mass terms:

$$\mathcal{L}_{\text{mass}} = -(\nu_e, \nu_\mu, \nu_\tau) \mathcal{M}_D \begin{pmatrix} N_e^c \\ N_\mu^c \\ N_\tau^c \end{pmatrix} - \frac{1}{2} (N_e^c, N_\mu^c, N_\tau^c) \mathcal{M}_R \begin{pmatrix} N_e^c \\ N_\mu^c \\ N_\tau^c \end{pmatrix} + \text{h.c.} , \quad (2)$$

where ν_α are the SM neutrinos of lepton flavour α , \mathcal{M}_D is the Dirac mass matrix and \mathcal{M}_R is the Majorana mass matrix given by,

$$\mathcal{M}_D = \frac{v}{\sqrt{2}} \begin{pmatrix} \lambda_e & 0 & 0 \\ 0 & \lambda_\mu & 0 \\ 0 & 0 & \lambda_\tau \end{pmatrix} , \quad \mathcal{M}_R = \begin{pmatrix} \lambda_{ee} \langle \Phi \rangle & \lambda_{e\mu} \langle \sigma_\mu \rangle & \lambda_{e\tau} \langle \sigma_\tau \rangle \\ \lambda_{e\mu} \langle \sigma_\mu \rangle & 0 & \lambda_{\mu\tau} \langle \Phi \rangle \\ \lambda_{e\tau} \langle \sigma_\tau \rangle & \lambda_{\mu\tau} \langle \Phi \rangle & 0 \end{pmatrix} , \quad (3)$$

respectively. We can simplify our analysis by choosing the $U(1)_{L_\mu - L_\tau}$ breaking VEVs, $\langle \sigma_\mu \rangle$ and $\langle \sigma_\tau \rangle$, to be real and positive through field redefinitions without loss of generality. Additionally, we can make the Dirac Yukawa couplings λ_e , λ_μ , and λ_τ real and positive. These Yukawa couplings can be parameterized as:

$$(\lambda_e, \lambda_\mu, \lambda_\tau) = \lambda (\cos \theta, \sin \theta \cos \phi, \sin \theta \sin \phi) , \quad (4)$$

where $0 < \lambda \leq 1$, and $0 \leq \theta, \phi \leq \pi/2$.

The light neutrino mass matrix is obtained from the Type-I seesaw formula [4–7],

$$\mathcal{M}_\nu = -\mathcal{M}_D \mathcal{M}_R^{-1} \mathcal{M}_D^T . \quad (5)$$

Since it is a complex symmetric matrix, it can be diagonalized with a unitary matrix as $U^T \mathcal{M}_\nu U = \text{diag}(m_1, m_2, m_3)$, where the unitary matrix U is the Pontecorvo-Maki-Nakagawa-Sakata (PMNS) neutrino mixing matrix and is given by

$$U = \begin{pmatrix} c_{12}c_{13} & s_{12}c_{13} & s_{13}e^{-i\delta} \\ -s_{12}c_{23} - c_{12}s_{23}s_{13}e^{i\delta} & c_{12}c_{23} - s_{12}s_{23}s_{13}e^{i\delta} & s_{23}c_{13} \\ s_{12}s_{23} - c_{12}c_{23}s_{13}e^{i\delta} & -c_{12}s_{23} - s_{12}c_{23}s_{13}e^{i\delta} & c_{23}c_{13} \end{pmatrix} \begin{pmatrix} 1 \\ e^{i\frac{\alpha_2}{2}} \\ e^{i\frac{\alpha_3}{2}} \end{pmatrix} , \quad (6)$$

where $c_{ij} \equiv \cos \theta_{ij}$ and $s_{ij} \equiv \sin \theta_{ij}$ with the mixing angles θ_{ij} , and we denote the Dirac CP phase and Majorana CP phases as δ , α_2 , and α_3 , respectively.

³We adopt a two-component spinor notation (see, e.g., Ref. [56]) as in Ref. [18].

⁴We assume that the scalar potential can be expressed as $V(H, \sigma_\mu, \sigma_\tau, \Phi) = V(H) + V(\sigma_\mu) + V(\sigma_\tau) + V(\Phi)$. We will present the explicit form of the scalar potential $V(\Phi)$ that we considered in Sec. 3.2.

Diagonalizing the Majorana mass matrix, we obtain the masses of right-handed neutrinos,

$$\mathcal{M}_R = \Omega^* \text{diag}(M_1, M_2, M_3) \Omega^\dagger, \quad (7)$$

where Ω is a unitary matrix and $M_{1,2,3}$ are the right-handed neutrino mass and they satisfy $0 < M_1 < M_2 < M_3$.

We note that in our model, the phases of the PMNS neutrino mixing matrix and the sum of the standard model neutrino masses are predictable by other neutrino oscillation parameters, because of restricted neutrino mass matrix structure in Eq. (3), so-called two-zero minor structure [15–20]. (This structure also appear in the $U(1)_{L_\mu-L_\tau}$ model with one singlet scalar, called the minimal gauged $U(1)_{L_\mu-L_\tau}$ model [18–20, 53–55].) Consequently, by fixing the three Dirac Yukawa couplings, we can determine each component of the Majorana mass matrix through the seesaw mechanism formula (5):

$$\mathcal{M}_R = -\mathcal{M}_D^T \mathcal{M}_\nu^{-1} \mathcal{M}_D. \quad (8)$$

Here, \mathcal{M}_ν is entirely determined by observed neutrino oscillation parameters. This implies that we have only three free input parameters λ , θ , and ϕ in the neutrino sector to establish the mass spectrum of right-handed neutrinos and their interactions with standard model particles. As an illustrative example, we present a contour plot (Fig 1) in the $\phi - \theta$ plane for each component of the Majorana mass matrix, denoted as $M_{ee} := \lambda_{ee} \langle \Phi \rangle$, $M_{e\mu} := \lambda_{e\mu} \langle \sigma_\mu \rangle$, $M_{e\tau} := \lambda_{e\tau} \langle \sigma_\tau \rangle$, and $M_{\mu\tau} := \lambda_{\mu\tau} \langle \Phi \rangle$, while fixing λ . We note that that relationships derived from Eq. (8) reveal that $M_{ee} \propto \lambda^2 \cos^2 \theta$, $M_{e\mu} \propto \lambda^2 \sin \theta \cos \theta \cos \phi$, $M_{e\tau} \propto \lambda^2 \sin \theta \cos \theta \sin \phi$, and $M_{\mu\tau} \propto \lambda^2 \sin^2 \theta \sin \phi \cos \phi$.

This analysis utilizes neutrino oscillation data from the NuFit analyses [57], which are comprehensive global fits that include data from all the relevant neutrino oscillation experiments. The most recent NuFit analyses (NuFit 5.2 [57, 58]) are conducted both with and without incorporating data from the Super-Kamiokande (SK) experiment. While these approaches yield different values for the neutrino mixing angles and squared mass differences, in Fig 1, we use without SK data as a representative to determine the light neutrino mass matrix \mathcal{M}_ν . We note that, to circumvent the constraint on the sum of light neutrino masses, $\sum_i m_i < (0.12 - 0.69) \text{ eV}$ [59, 60] (see also Refs. [61–66]), we set θ_{23} within the $+3\sigma$ range (detailed in Ref. [22]).

In this study, we focus on the scenario where the breaking scale of $U(1)_{L_\mu-L_\tau}$ is lower than that of the electroweak phase transition, or more precisely, the temperature at which sphaleron processes freeze out. We make the assumption that the vacuum expectation value (VEV) of the $U(1)_{B-L}$ breaking scalar field, Φ , is significantly larger than the Higgs VEV:

$$\langle \sigma_\mu \rangle, \langle \sigma_\tau \rangle < v/\sqrt{2} \ll \langle \Phi \rangle, \quad (9)$$

Such a low $U(1)_{L_\mu-L_\tau}$ breaking scale gives rise to a light $U(1)_{L_\mu-L_\tau}$ gauge boson since its mass is determined by the $U(1)_{L_\mu-L_\tau}$ breaking VEV: $m_{Z'} = 2g' \langle \sigma \rangle$. Here and in what follows, we denote the $U(1)_{L_\mu-L_\tau}$ breaking scale as $\langle \sigma \rangle := \sqrt{(\langle \sigma_\mu \rangle)^2 + (\langle \sigma_\tau \rangle)^2}/2$, and refer to the mass and coupling of Z' as $m_{Z'}$ and g' , respectively. The light $U(1)_{L_\mu-L_\tau}$ gauge boson is motivated by various phenomenology including the muon $g-2$ anomaly [23–27], Hubble tension [28, 29], and the search for dark sector particles [30, 31]. Particularly in

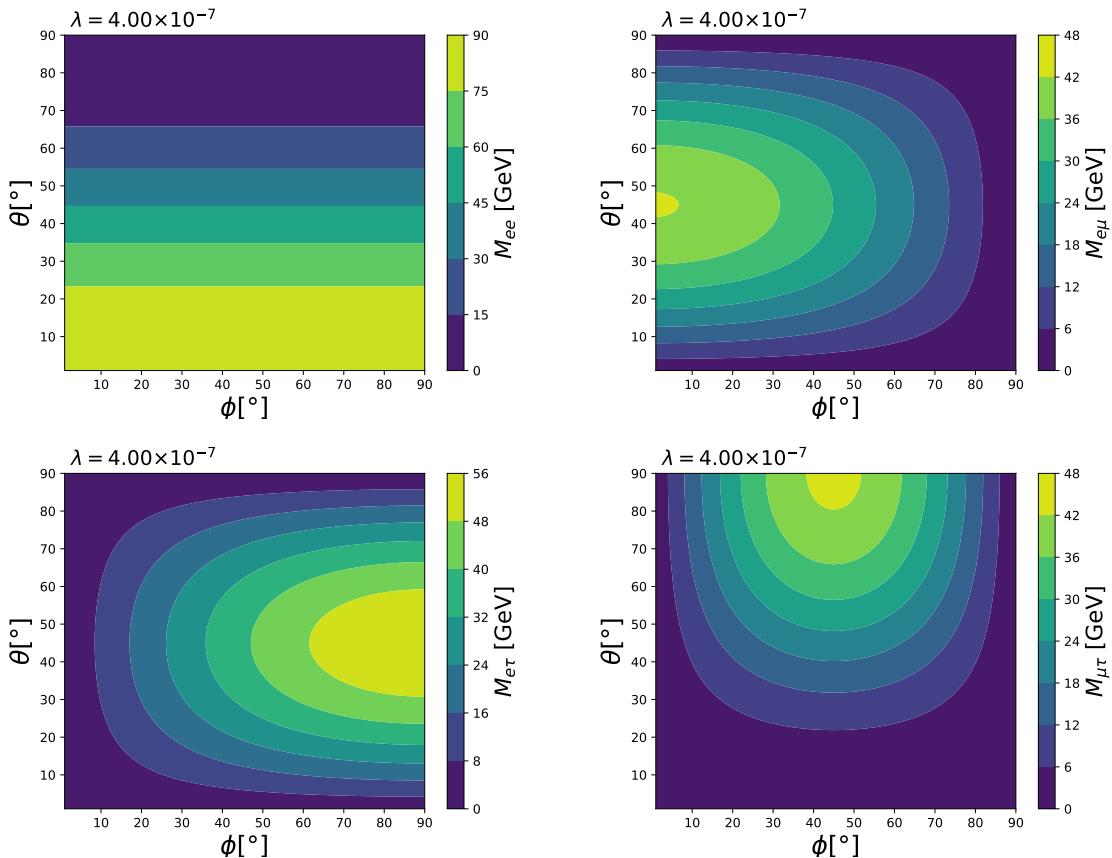


Figure 1: Contours in the $\phi - \theta$ plane illustrating the dependence of each component of the Majorana mass matrix on the model parameters. The plots depict $M_{ee} := \lambda_{ee} \langle \Phi \rangle$ (top left), $M_{e\mu} := \lambda_{e\mu} \langle \sigma_\mu \rangle$ (top right), $M_{e\tau} := \lambda_{e\tau} \langle \sigma_\tau \rangle$ (bottom left), and $M_{\mu\tau} := \lambda_{\mu\tau} \langle \Phi \rangle$ (bottom right). Here, we choose $\lambda = 4 \times 10^{-7}$ for subsequent discussions, and utilize neutrino oscillation parameters from the NuFit 5.2 analysis [57, 58] (without SK data). Note that relationships derived from Eq. (8) reveal that $M_{ee} \propto \lambda^2 \cos^2 \theta$, $M_{e\mu} \propto \lambda^2 \sin \theta \cos \theta \cos \phi$, $M_{e\tau} \propto \lambda^2 \sin \theta \cos \theta \sin \phi$, and $M_{\mu\tau} \propto \lambda^2 \sin^2 \theta \sin \phi \cos \phi$.

the region favored by the muon $g - 2$ anomaly, the expected $U(1)_{L_\mu - L_\tau}$ breaking scale is $\langle \sigma \rangle = 10 - 50$ GeV [67].⁵

As illustrated in Fig 1, within the central region on the $\phi - \theta$ plane, each component of the Majorana mass matrix exhibits comparable values. This implies a hierarchy among the Yukawa couplings in the Majorana mass matrix, given by:

$$\lambda_{ee}, \lambda_{\mu\tau} \ll \lambda_{e\mu}, \lambda_{e\tau}. \quad (10)$$

Hereafter, we make the assumption that the Yukawa couplings associated with the $U(1)_{L_\mu - L_\tau}$ breaking scalar are not significantly small, namely $\lambda_{e\mu}, \lambda_{e\tau} \sim \mathcal{O}(0.1 - 1)$, while the couplings with the $U(1)_{B-L}$ breaking scalar are substantially smaller.

⁵Several experiments have already ruled out specific regions within the parameter space where the gauged $U(1)_{L_\mu - L_\tau}$ model could potentially explain the observed muon $g - 2$ anomaly [68–72]. More recently, the NA64 μ experiment presented the results, further constraining the remaining $(m_{Z'}, g_{Z'})$ parameter space [67]. By combining these experimental constraints, we identify a small allowed region characterized by $m_{Z'} \sim 1 - 4 \times 10^{-2}$ GeV and $g' \sim 4 - 5 \times 10^{-4}$, leading to $\langle \sigma \rangle = 10 - 50$ GeV.

In our model, as elucidated thus far, each components in the Majorana mass term are parameterized by three parameters, (λ, θ, ϕ) and their magnitudes scale with λ^2 . Therefore, once we fix (λ, θ, ϕ) , it determines $M_{e\mu} = \lambda_{e\mu} \langle \sigma_\mu \rangle$ and $M_{e\tau} = \lambda_{e\tau} \langle \sigma_\tau \rangle$ components related to the $U(1)_{L_\mu-L_\tau}$ breaking scale and vice versa. Indeed, the breaking scale favored by the muon $g-2$ anomaly yields a range of λ , with $\lambda \lesssim 5 \times 10^{-7}$ in the central region of the $\phi - \theta$ plane.

At high temperatures, symmetry broken by scalar VEVs could be restored due to thermal effects and finite density effects [38]. In the $U(1)_{L_\mu-L_\tau}$ symmetric phase, the Majorana mass matrix takes the form:

$$\mathcal{M}_{R,\text{sym}} = \begin{pmatrix} \lambda_{ee} \langle \Phi \rangle & 0 & 0 \\ 0 & 0 & \lambda_{\mu\tau} \langle \Phi \rangle \\ 0 & \lambda_{\mu\tau} \langle \Phi \rangle & 0 \end{pmatrix}, \quad (11)$$

where $\mathcal{M}_{R,\text{sym}}$ indicates the Majorana mass matrix in the $U(1)_{L_\mu-L_\tau}$ symmetric phase. Since most of the components in the neutrino mass matrix are restricted from $U(1)_{L_\mu-L_\tau}$ symmetry, we lack sufficient physical phases in the $U(1)_{L_\mu-L_\tau}$ symmetric phase. As discussed in Ref. [38], this deficit can lead to the failure of the leptogenesis scenario if the breaking of $U(1)_{L_\mu-L_\tau}$ symmetry occurs subsequent to the decoupling of the sphaleron processes. This limitation arises because the production of lepton asymmetry becomes unattainable after the temperature at which the sphaleron processes decouple, denoted as T_{sph} . The condition $T_{\text{bre}} < T_{\text{sph}}$, where $T_{\text{bre}} \simeq \langle \sigma \rangle$, is satisfied for $\lambda \lesssim 8 \times 10^{-7}$ for the parameter point located in the central region of the $\phi - \theta$ plane. We note that the breaking scale of the $U(1)_{L_\mu-L_\tau}$ symmetry is approximately determined by λ in our model, as previously mentioned.

However, in the following section, we will demonstrate that the introduction of a $U(1)_{B-L}$ breaking scalar, denoted as Φ , and the assumption of kinetic misalignment of Φ in the early universe can resolve this issue. This is because the kinetic motion of the scalar field can dynamically generate the CP phase, as in the Affleck-Dine mechanism [39, 40]. While our scenario draws inspiration from the recent work [51], we incorporate different phenomenological aspects, as elucidated below.

3 Leptogenesis driven by majoron rotation

In this section, we will discuss leptogenesis in the $U(1)_{L_\mu-L_\tau}$ symmetric phase, and evaluate the produced baryon asymmetry and dark matter abundance in our model.

3.1 Brief overview

Firstly, we briefly explain how to realize successful leptogenesis in the $U(1)_{L_\mu-L_\tau}$ symmetric phase. Hereafter, we parameterize the $U(1)_{B-L}$ breaking field as

$$\Phi = \frac{1}{\sqrt{2}} (S + f) e^{i\chi/f}, \quad (12)$$

where S represents the radial mode and χ is the majoron field. (Here, $\langle \Phi \rangle = f/\sqrt{2}$.) The $B-L$ charge in the scalar sector, denoted as n_{B-L} , is given as $n_{B-L} := 2i(\Phi\dot{\Phi}^* - \dot{\Phi}\Phi^*)$,

with a dot indicating a time derivative. After the radial component of the singlet scalar Φ has settled to the minimum, the $B - L$ charge asymmetry can be expressed as

$$n_{B-L} = 2\dot{\Theta}f^2, \quad (13)$$

where $\Theta := \chi/f$.

Suppose that the non-zero $\dot{\Theta}$ background is induced from the rotation of the complex scalar Φ in the early universe. This situation can be realized through the kinetic misalignment mechanism [41–43]⁶. As long as this rotation persists, $B - L$ charge is stored in the scalar sector, with a portion of this charge contributing to lepton asymmetry through interactions between right-handed neutrinos and leptons [51]. Importantly, even without a CP-violating decay process, lepton asymmetry can be produced. This is because the dynamical background field, the majoron χ , dynamically introduces the CP phase. This becomes evident when we redefine fermionic fields $\psi \rightarrow \psi e^{i(B-L)_\psi\Theta/2}$, where $(B - L)_\psi$ denotes the $B - L$ number of the particle ψ (See Table 1). As a consequence of this redefinition, we can eliminate the majoron field (or Θ dependence) in the original Lagrangian, and the derivative coupling with the majoron remains, i.e. $-\partial_\mu\Theta J_{B-L}^\mu/2$, where J_{B-L}^μ is the $B - L$ current. This derivative coupling to the majoron induces level splittings between leptons and anti-leptons [45, 51], which leads to deviation of the thermal averaged interaction rate between the lepton number violating process and the inverse process [45]. This deviation causes an external chemical potential [45, 51], which can be converted to lepton asymmetry via Yukawa interaction of right-handed neutrinos with leptons and Higgs. Therefore, this mechanism offers a solution to the challenge of leptogenesis in the $U(1)_{L_\mu-L_\tau}$ symmetric phase, addressing the lack of a CP phase in the neutrino sector. The produced lepton asymmetry will be transformed into baryon asymmetry via the sphaleron process. It should be noted that this dynamic level splitting violates the CPT-invariance and hence baryon asymmetry can be generated without satisfying Sakharov’s conditions exactly [45].

A similar mechanism was initially proposed in the recent paper [51], wherein the authors considered a model with purely global $U(1)_{B-L}$ symmetry and assumed the absence or substantial suppression of CP-violating decay of right-handed neutrinos. In contrast, our work explores a model that features both gauged $U(1)_{L_\mu-L_\tau}$ and global $U(1)_{B-L}$ symmetries. Consequently, i) the lack of a CP phase arises due to the restriction imposed by gauge symmetry rather than as an assumption. ii) Our model retains predictivity for neutrino oscillation parameters such as the phase of the PMNS matrix and the sum of light neutrino masses due to gauge symmetry constraints. iii) The mass spectrum of right-handed neutrinos and their interactions with standard model particles are entirely determined by three parameters: λ , θ , and ϕ . This determination remains valid even in the $U(1)_{L_\mu-L_\tau}$ symmetric phase. Moreover, we emphasize that our scenario provides a solution for realizing leptogenesis in the $U(1)_{L_\mu-L_\tau}$ symmetric phase.

⁶ The non-zero $\dot{\Theta}$ background could also be induced from majoron oscillation. This mechanism is called spontaneous leptogenesis [45, 51]. (See also Ref. [44, 46]) However, to generate a sufficient amount of baryon asymmetry, a much heavier right-handed neutrino mass $M_i > 10^{10}$ GeV is required [45, 51]. In contrast, in this work, we consider a lower mass scale $M_i \sim O(10 - 100)$ GeV.

3.2 Evaluation of baryon asymmetry and dark matter abundance

Next, we evaluate the expected baryon asymmetry in our model. As a first step, we estimate the $B - L$ charge in the scalar sector, n_{B-L} , by following Refs. [41, 43, 47]. After that, we compute the baryon asymmetry and dark matter density produced by our model.

In this study, we employ the quartic potential previously demonstrated in Refs. [41, 43, 47], given by:

$$V(\Phi) = \kappa^2 \left(|\Phi|^2 - \frac{f^2}{2} \right)^2, \quad \kappa^2 = \frac{1}{2} \frac{m_S^2}{f^2}. \quad (14)$$

Here, m_S represents the vacuum mass of the radial mode of S . We assume that cross terms with other scalars (e.g., $|\Phi|^2|H|^2$, $|\Phi|^2|\sigma_\mu|^2$, and $|\Phi|^2|\sigma_\tau|^2$, etc.) are negligible. Additionally, we assume a large initial field value $|\Phi_i| = S_i/\sqrt{2} \gg f$, which is permissible when the quartic coupling is sufficiently small, indicative of a flat potential for S .⁷ The radial component initiates oscillations when the Hubble friction weakens compared to the curvature of the quartic potential, given by $3H(T_{S,\text{osc}}) \simeq \sqrt{3}\kappa S_i$. Suppose that the universe is a radiation-dominated universe at this stage. Then this condition yields $T_{S,\text{osc}}$ as⁸:

$$T_{S,\text{osc}} \simeq \left(\frac{30}{\pi^2 g_*} \right)^{1/4} \sqrt{\kappa M_{\text{pl}} S_i}, \quad (15)$$

where g_* represents the effective degrees of freedom, and M_{pl} denotes the reduced Planck mass. We note that $H(T_{\text{osc}})$ is constrained by the upper limit of the Hubble parameter during inflation, $H_{\text{inf}} \lesssim 2.5 \times 10^{-5} M_{\text{pl}}$ [74]. This constraint yields

$$\kappa \lesssim 2.5\sqrt{3} \times 10^{-5} \left(\frac{M_{\text{pl}}}{S_i} \right) \quad (16)$$

or, equivalently, $m_S/f \lesssim 2.5\sqrt{6} \times 10^{-5} (M_{\text{pl}}/S_i)$.

To produce $B - L$ asymmetry, we introduce explicit global symmetry breaking through a higher-dimensional operator:

$$V(\Phi)_{B-L} = c_n \frac{\Phi^n}{M^{n-4}} + h.c., \quad (17)$$

where M is a cut-off parameter and c_n is a coefficient of this term. For large S_i , this term gives a kick to the phase direction of the scalar Φ and causes the rotation. As S decreases, the explicit breaking effect diminishes, and the effect can be rephrased in terms of majoron mass, which can be estimated as follows:

$$m_\chi \simeq \frac{n}{2^{(n-2)/4}} \left(|c_n| \frac{f^{n-2}}{M^{n-4}} \right)^{1/2}. \quad (18)$$

⁷The flat potential naturally arises in supersymmetric theories and plays an essential role in the Affleck-Dine mechanism [39, 40]. In supersymmetric theories, the large field value may arise during inflation due to the negative Hubble-induced mass term [40, 73]. In this paper, supersymmetry is not necessarily assumed. See Refs. [41, 43, 47] for detailed discussions and evaluations of the $U(1)$ charge in the scalar sector in supersymmetric theories.

⁸The evaluation for the case that S dominates the universe is given in Refs. [41, 43], in details.

Due to this potential curvature at the minimum, the $B-L$ charge might undergo a slight change after Φ reaches its minimum. However, for $|\Phi| \sim f$, this effect is suppressed by a factor of $(f/S_i)^n$ relative to the effect at $|\Phi| \sim S_i$. Therefore, in this paper, we neglect this effect and treat n_{B-L} as an approximately conserved charge during leptogenesis.

If the universe remains radiation-dominated throughout its evolution, the $B-L$ charge density normalized by the entropy density, denoted as $Y_{B-L} := n_{B-L}/s$, remains constant in the expanding universe. It is given by [41, 43, 47]

$$Y_{B-L} = \epsilon \frac{V(\Phi_i)}{s(T_{S,\text{osc}}) m_S(\Phi_i)} = \epsilon \left(\frac{\pi^2 g_*}{30} \right)^{\frac{3}{4}} \frac{15\sqrt{3}}{4\pi^2 g_*} \frac{S_i^{3/2}}{\sqrt{\kappa} M_{\text{pl}}^{3/2}}, \quad (19)$$

where Φ_i represents the initial field configuration of Φ , and ϵ is defined as the ratio of the number density of phase component $n_{B-L}/2$ to the number density of the radial component n_S :

$$\epsilon := \frac{n_{B-L}}{2n_S}, \quad (20)$$

with $0 < \epsilon < 1$ by definition. To evaluate ϵ , we can derive the following expression for the $B-L$ asymmetry at time t using the equation of motion for Φ [47]:

$$R^3 n_{B-L} = 4n \int R^2 \text{Im} \left[c_n \frac{\Phi^n}{M^{n-4}} \right] \frac{dR}{H}, \quad (21)$$

where R denotes the scale factor. Initially, $|\Phi|$ remains frozen due to Hubble friction, resulting in a constant field value $S = S_i$. In a radiation-dominated universe, the term on the right-hand side becomes proportional to R^5 , making its dominant contribution evident at later times. After $3H \simeq \sqrt{3}\kappa S_i$, the time when field S starts oscillating, its amplitude begins to decrease. Consequently, the contribution to the $B-L$ asymmetry diminishes at later times. This leads to the effective conservation of the number density n_{B-L} , as $V(\Phi)_{B-L}$ becomes insignificant. Thus, the $B-L$ asymmetry is predominantly generated at the initiation of S oscillations at $R = R_{\text{osc}}$, and can be approximated by evaluating the integral at R_{osc} [47]:

$$n_{B-L}(t_{\text{osc}}) \simeq \frac{4\sqrt{3}n |c_n| S_i^n \delta_{\text{eff}}}{2^{n/2} M^{n-4} \kappa S_i}, \quad (22)$$

$$\delta_{\text{eff}} := \sin(n\Theta_{\text{osc}} + \arg[c_n]), \quad (23)$$

where Θ_{osc} represents the phase of Φ when its radial component begins to oscillate, and t_{osc} denotes the time corresponding to R_{osc} . From this analysis, the expression for ϵ is given by

$$\epsilon \simeq \frac{24n}{2^{n/2}} \frac{|c_n|}{M^{n-4}} \frac{S_i^{n-4}}{\kappa^2} \delta_{\text{eff}} \quad (24)$$

$$\simeq \frac{24}{n} \frac{m_\chi^2}{m_S^2} \frac{S_i^{n-4}}{f^{n-4}} \delta_{\text{eff}}, \quad (25)$$

where the case for $\epsilon > 1$ may seem unphysical. In reality, when the effects of higher-dimensional terms are significant, the phase degree of freedom reaches its minimum before

the radial component begins to oscillate. Specifically, $\Theta_{\text{osc}} \rightarrow (-\arg[c_n] + (2m + 1)\pi)/n$ (where $m = 0, 1, 2, \dots$). As a result, the originally $O(1)$ value of δ_{eff} vanishes, the rotation is suppressed, and $\epsilon \sim 0$. Therefore, in practice, $\epsilon > 1$ will not be achieved. A more detailed quantitative estimation is deferred to the subsequent discussion.

We now discuss the constraint imposed by the higher-dimensional operator introduced in Eq. (17). Generally, such an operator can potentially induce an unwanted minimum in the potential of Φ and may spoil this mechanism. This risk arises because the scalar field Φ possesses a large initial field value and might eventually settle into this minimum [75, 76]. To circumvent this issue, at the onset of oscillations, the curvature in the phase direction needs to be smaller than the Hubble parameter. This condition is given by the following expression [76]:

$$m_{\chi, \text{eff}}(S_i) \lesssim H(T_{\text{S,osc}}), \quad (26)$$

where $m_{\chi, \text{eff}}(S_i) := m_{\chi}(S_i/f)^{(n-2)/2}$. This condition can also be interpreted as the requirement, that the mass of the radial mode evaluated at the large initial field value S_i should be larger than the mass of the angular mode evaluated at S_i , which is the condition for the validity of the Nambu-Goldstone treatment [49].

For the quartic potential given by Eq. (14), this condition simplifies to the upper limit on the majoron mass,

$$m_{\chi} \lesssim 10^{23-5n} \text{ GeV} \left(\frac{\kappa}{10^{-5}} \right) \left(\frac{S_i}{M_{\text{pl}}} \right)^{-\frac{n-2}{2}} \left(\frac{f}{10^8 \text{ GeV}} \right)^{\frac{n-2}{2}} \left(\frac{10^{18} \text{ GeV}}{M_{\text{pl}}} \right)^{\frac{n-4}{2}}. \quad (27)$$

For the cases $n = 5$ and $n = 6$, this yields $m_{\chi} \lesssim 10 \text{ MeV}$ and $m_{\chi} \lesssim 100 \text{ eV}$ respectively, for $f \simeq 10^8 \text{ GeV}$ and $\kappa \simeq 10^{-5}$. This constraint, Eq. (26), also establishes an upper limit on ϵ as

$$\epsilon \lesssim \frac{4}{n} \delta_{\text{eff}}, \quad (28)$$

from Eq. (25). Therefore, ϵ cannot be arbitrarily large. In general, the larger the value of n , the more stringent the constraints on ϵ become. If parameters that do not satisfy this constraint are chosen, the phase direction will reach its minimum before the radial direction, as mentioned above, resulting in $\delta_{\text{eff}} \ll 1$ and hindering the rotation.

If the right-handed neutrinos are in the thermal bath, the non-zero $\dot{\Theta}$ background or equivalently, the produced $B-L$ asymmetry in the scalar sector, causes lepton asymmetry in the SM sector through the Yukawa interaction of the right-handed neutrino. To analyze this, we diagonalize the Majorana mass term in the $U(1)_{L_{\mu}-L_{\tau}}$ symmetric phase (11) as

$$\mathcal{L}_N = -\hat{\lambda}_{i\alpha} \hat{N}_i^c (L_{\alpha} \cdot H) - \frac{1}{2} M_i^{\text{sym}} \hat{N}_i^c \hat{N}_i^c + \text{h.c.}, \quad (29)$$

where,

$$\mathcal{M}_{R, \text{sym}} = \Omega_{\text{sym}}^* \text{diag}(M_1^{\text{sym}}, M_2^{\text{sym}}, M_3^{\text{sym}}) \Omega_{\text{sym}}^{\dagger}, \quad (30)$$

$$\hat{N}_i^c = \sum_{\alpha} \Omega_{\text{sym}, \alpha i}^* N_{\alpha}^c, \quad (31)$$

$$\hat{\lambda}_{i\alpha} = \Omega_{\text{sym}, \alpha i} \lambda_{\alpha} \text{ (not summed)}, \quad (32)$$

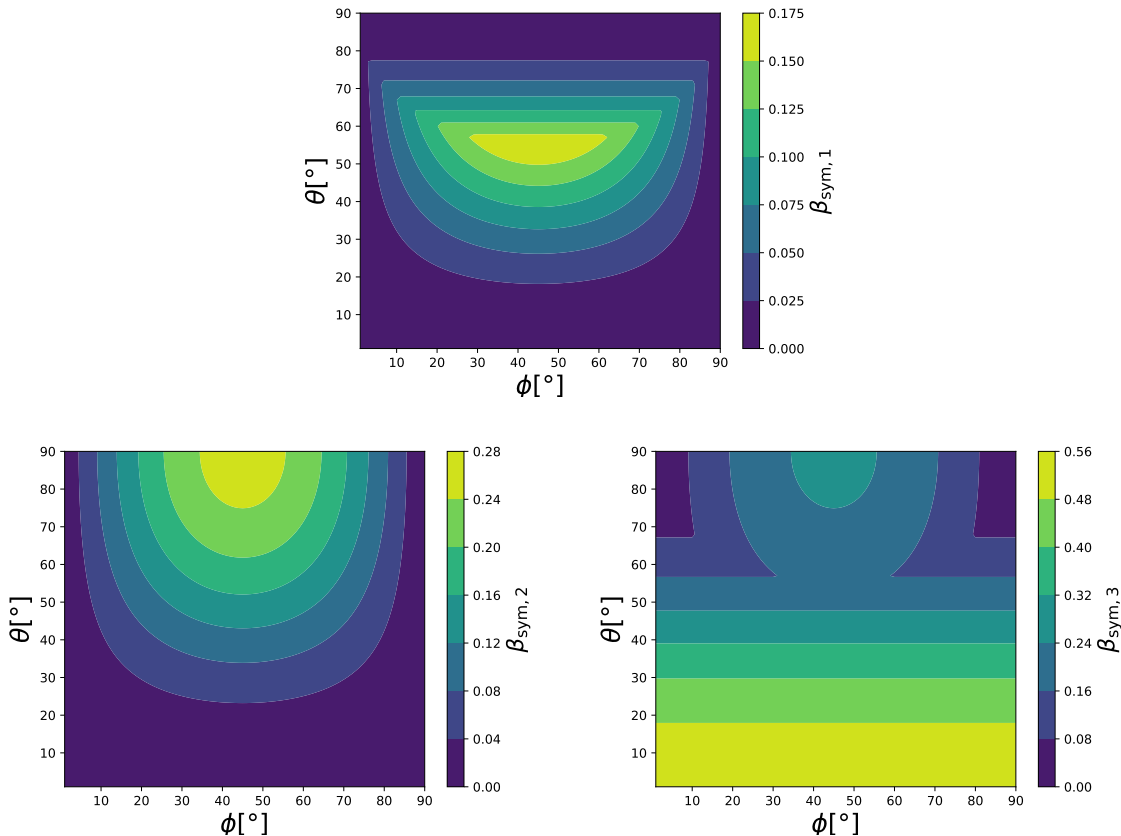


Figure 2: Contour plots illustrating the behavior of the functions $\beta_{\text{sym},1}$ (top panel), $\beta_{\text{sym},2}$ (bottom left), and $\beta_{\text{sym},3}$ (bottom right). The input parameter values are consistent with those used in Fig. 1. It is noteworthy that for small values of θ , corresponding to a large M_{ee} , the mass of the heaviest right-handed neutrino M_3 can be approximated as $M_{ee} \propto \cos^2 \theta$ and remains independent of ϕ .

where Ω_{sym} is a unitary matrix that diagonalizes $\mathcal{M}_{R,\text{sym}}$, and $M_{1,2,3}^{\text{sym}}$ are the right-handed neutrino masses in the $U(1)_{L_\mu-L_\tau}$ symmetric phase.

It is worth noting that the components of the Majorana mass $\mathcal{M}_{R,\text{sym}}$, are equivalent to those of \mathcal{M}_R as defined in Eq. (3). Consequently, these components can be computed from the light neutrino mass matrix using Eq. (8). As a consequence, the masses of the right-handed neutrinos are proportional to λ^2 even in the symmetric phase. This dependence can be expressed more precisely as follows,

$$M_{1,2,3}^{\text{sym}} = \frac{v^2 \lambda^2}{2m_1} \beta_{\text{sym},1,2,3}, \quad (33)$$

where $\beta_{\text{sym},1,2,3}$ are real numbers satisfying $\beta_{\text{sym},1,2,3} \lesssim O(1)$. We present contour plots of $\beta_{\text{sym},1,2,3}$ in the $\phi - \theta$ plane in Fig. 2. These plots utilize the same neutrino oscillation parameters as in Fig. 1. As indicated in Eq. (11), the two mass eigenvalues are exactly degenerate, i.e., $M_1^{\text{sym}} < M_2^{\text{sym}} = M_3^{\text{sym}}$ or $M_1^{\text{sym}} = M_2^{\text{sym}} < M_3^{\text{sym}}$, depending on the values of θ and ϕ .

The decay width of the right-handed neutrino to the lepton and SM Higgs boson in

$U(1)_{L_\mu-L_\tau}$ symmetric phase is given by

$$\Gamma_{N_i \rightarrow l_\alpha H}^{\text{sym}} = \frac{1}{8\pi} (\hat{\lambda}_{i\alpha} \hat{\lambda}_{\alpha i}^*) M_i^{\text{sym}}, \quad (34)$$

and total decay width to the SM leptons is $\Gamma_{N_i \rightarrow lH}^{\text{sym}} := \sum_\alpha \Gamma_{N_i \rightarrow l_\alpha H}^{\text{sym}} = \frac{1}{8\pi} (\hat{\lambda} \hat{\lambda}^\dagger)_{ii} M_i^{\text{sym}}$. It is convenient to define the thermal averaged decay width as follows:

$$\langle \Gamma_{N_i \rightarrow l_\alpha H}^{\text{sym}} \rangle := \frac{K_1(z)}{K_2(z)} \Gamma_{N_i \rightarrow l_\alpha H}^{\text{sym}}, \quad (35)$$

with K_1 and K_2 are modified Bessel functions for 1st and 2nd kind, and $z := M_1^{\text{sym}}/T$.

In the presence of a non-zero $\dot{\Theta}$ background, the Boltzmann equation for the lepton asymmetry density $n_{\Delta l} := n_l - n_{\bar{l}}$ is modified as follows [48, 51]⁹:

$$\dot{n}_{\Delta l_\alpha} + 3H n_{\Delta l_\alpha} = - \sum_i n_{N_i}^{\text{eq}} \langle \Gamma_{N_i \rightarrow l_\alpha H}^{\text{sym}} \rangle \left(\frac{n_{\Delta l_\alpha}}{n_{l_\alpha}^{\text{eq}}} + \frac{n_{\Delta H}}{n_H^{\text{eq}}} - \frac{\dot{\Theta}}{T} \right), \quad (\alpha = e, \mu, \tau) \quad (36)$$

where $n_{\Delta H} := n_H - n_{\bar{H}}$, and n_X , ($X = l_\alpha, N, H$) represent the equilibrium number density of X . Here, we neglect the lepton number violating scattering term because they are a higher order of $\lambda \ll 1$. We briefly show the derivation of this Boltzmann equation in Appendix A.

Significantly, in our model during leptogenesis, the right-handed neutrinos are in thermal equilibrium, i.e., $n_{N_i} = n_{N_i}^{\text{eq}}$. Additionally, the absence of CP phases in the neutrino sector results in the lack of a decay term. Consequently, only terms corresponding to the inverse decay remain on the right-hand side of Eq. (36). As shown in Eq. (36), if inverse decay is in thermal equilibrium, the lepton asymmetry becomes:

$$n_{\Delta l} = \frac{c_L}{6} \dot{\Theta} T^2, \quad (37)$$

where c_L is the coefficient determined by the equations of chemical equilibrium. At low temperatures, $T < 10^5$ GeV, $c_L \simeq 51/22$ [51]. In comparison to the asymmetry in the scalar sector $n_{B-L} = 2\dot{\Theta} f^2$, the lepton asymmetry in the thermal bath is suppressed by the factor T^2/f^2 .

Since the production of lepton asymmetry in our model relies on the inverse decay of right-handed neutrinos, a strong washout condition is required for this mechanism. This condition is quantified by the decay parameter $K := \tilde{m}_1/m_* > 1$ [83], where $\tilde{m}_1 := (\hat{\lambda} \hat{\lambda}^\dagger)_{11} v^2 / 2M_1$, and $m_* \simeq 1 \times 10^{-3}$ eV represent the effective neutrino mass, and the equilibrium neutrino mass respectively. In our model, the lightest neutrino mass is on the order of the atmospheric neutrino mass, i.e., $m_1 \simeq O(0.05)$ eV, indicating that the effective mass \tilde{m}_1 is typically of the same order. Consequently, the strong washout condition is indeed satisfied with $K > 1$. To assess the baryon asymmetry, it is crucial to identify the temperature range where the inverse decay process of the right-handed neutrino is

⁹Since we focus on low-scale leptogenesis $M_i^{\text{sym}} \ll 10^5$ GeV, we neglect the heavy flavor effect [77–80] when evaluating baryon (lepton) asymmetry, while flavor effect is taken into account [77, 81, 82]. In our model, another type of flavor effect potentially exists, caused by $U(1)_{L_\mu-L_\tau}$ gauge bosons and Higgs bosons because they are also in the thermal bath. However, a detailed analysis of this effect goes beyond the scope of our paper.

in thermal equilibrium. To do this, it is convenient to define the following conventional function,

$$W_{\text{ID}}(z) := \frac{1}{2} \sum_i \frac{\langle \Gamma_{N_i \rightarrow lH}^{\text{sym}} \rangle n_{N_i}^{\text{eq}}}{H(z)z n_{l_\alpha}^{\text{eq}}}, \quad (38)$$

which parametrizes whether inverse right-handed neutrino decay is in thermal equilibrium or not, that is, if $W_{\text{ID}}(z) > 1$, the inverse right-handed neutrino decay is in thermal equilibrium. In our scenario, we focus on the centered region in the $\theta - \phi$ plane, where the mass eigenvalue of each right-handed neutrino is in the same scale, $M_1 \simeq M_2 \simeq M_3$, and also, the decay rate is approximately same as well. Therefore, $W_{\text{ID}}(z)$ can be approximately evaluated by

$$\begin{aligned} W_{\text{ID}}(z) &\simeq \frac{3}{2} \frac{\langle \Gamma_{N_1 \rightarrow lH}^{\text{sym}} \rangle n_{N_1}^{\text{eq}}}{H(z)z n_{l_\alpha}^{\text{eq}}} \\ &= \frac{3}{4} K z^3 K_1(z). \end{aligned} \quad (39)$$

Given a fixed value of K , the condition $W_{\text{ID}}(z) > 1$ leads to the range:

$$M_1^{\text{sym}}/z_{\text{out}} \lesssim T \lesssim M_1^{\text{sym}}/z_{\text{in}}, \quad (40)$$

where z_{in} and z_{out} represent the minimum and maximum values of z at which the inverse right-handed neutrino decay is in thermal equilibrium, respectively. Therefore, leptogenesis occurs in the interval $z_{\text{in}} < z < z_{\text{out}}$ within our model. We have numerically computed these values for our benchmark points and found that $M_1^{\text{sym}}/z_{\text{in}} > T_{\text{sph}}$ is satisfied for these points, as we will explain in the subsequent section.

Finally, the lepton asymmetry in the thermal bath will be converted to the baryon asymmetry via the sphaleron process. Assuming the right-handed neutrino inverse decay is in thermal equilibrium during leptogenesis, the resulting baryon asymmetry $Y_B := n_B/s$ is fixed at the temperature where the sphaleron process freezes out. For the case $n = 5$, the evaluation of Y_B is given by

$$\begin{aligned} Y_B &= \frac{1}{6} c_B Y_{B-L} \left(\frac{T_{\text{sph}}}{f} \right)^2 \\ &\simeq 9 \times 10^{-11} \left(\frac{\delta_{\text{eff}}}{1} \right) \left(\frac{T_{\text{sph}}}{130 \text{ GeV}} \right)^2 \left(\frac{S_i}{M_{\text{pl}}} \right)^{5/2} \\ &\quad \times \left(\frac{M_{\text{pl}}}{2.4 \times 10^{18} \text{ GeV}} \right) \left(\frac{10^{-2} \text{ GeV}}{m_S} \right)^{5/2} \left(\frac{m_\chi}{0.5 \text{ eV}} \right)^2 \left(\frac{10^7 \text{ GeV}}{f} \right)^{5/2}, \end{aligned} \quad (41)$$

and for the case $n = 6$,

$$\begin{aligned} Y_B &= \frac{1}{6} c_B Y_{B-L} \left(\frac{T_{\text{sph}}}{f} \right)^2 \\ &\simeq 9 \times 10^{-11} \left(\frac{\delta_{\text{eff}}}{1} \right) \left(\frac{T_{\text{sph}}}{130 \text{ GeV}} \right)^2 \left(\frac{S_i}{M_{\text{pl}}} \right)^{7/2} \\ &\quad \times \left(\frac{M_{\text{pl}}}{2.4 \times 10^{18} \text{ GeV}} \right)^2 \left(\frac{2 \times 10^{-2} \text{ GeV}}{m_S} \right)^{5/2} \left(\frac{m_\chi}{0.05 \text{ meV}} \right)^2 \left(\frac{3 \times 10^8 \text{ GeV}}{f} \right)^{7/2}, \end{aligned} \quad (42)$$

where c_B is a temperature-dependent coefficient, Y_{B-L} is given by Eq (19), and δ_{eff} is defined in Eq. (23). We have used the value c_B at low temperatures, specifically $T < 10^5$ GeV, which is $c_B = -(28/22)$ [51]. We have also used Eq. (24) to evaluate the ϵ . In the next section, we will present the parameter region capable of producing the correct baryon asymmetry in Fig 3. If the right-handed neutrino is too light such that $M_1^{\text{sym}}/z_{\text{in}} < T_{\text{sph}}$, the inverse decay is not in thermal equilibrium at the sphaleron decoupling temperature, hence baryon asymmetry is produced through the freeze-in mechanism. In this case, we have an additional suppression factor, expected to be $\sim W_{\text{ID}}(z_{\text{sph}})z_{\text{sph}}$, where $z_{\text{sph}} = M_1^{\text{sym}}/T_{\text{sph}}$ [51, 52]. We need to care about this effect when $M_1^{\text{sym}} \lesssim 20$ GeV.

Next, we evaluate the dark matter abundance within the context of our model. In our model, the abundance of dark matter is generated through the coherent oscillation of the majoron.¹⁰ In contrast to the conventional misalignment mechanism [84–86], the majoron field has the initial energy of kinetic motion in our model. This delays the epoch of majoron oscillation until the kinetic energy becomes comparable to the potential energy of the majoron. This mechanism is termed the kinetic misalignment mechanism [41–43].

After sphaleron freezes out, the kinetic energy of the majoron field decreases as $f^2\dot{\Theta}^2/2 \propto T^6$ because $n_{B-L} = 2f^2\dot{\Theta} \propto T^3$. Eventually, the majoron field fails to overcome the potential barrier induced by the higher-dimensional operator expressed in Eq. (17) on the bottom, resulting in the cessation of rotation. We denote this temperature as T_{trap} , determined by $f^2\dot{\Theta}^2(T_{\text{trap}})/2 \simeq m_\chi^2 f^2$. In the conventional misalignment mechanism, the majoron field starts to oscillate coherently when $3H(T_{\chi,\text{osc}}) \simeq m_\chi$. However, if $T_{\text{trap}} < T_{\chi,\text{osc}}$, the oscillation starts at the T_{trap} rather than $T_{\chi,\text{osc}}$. Notably, T_{trap} depends on the generated baryon asymmetry:

$$s(T_{\text{trap}}) \simeq \frac{2f^2 m_\chi}{Y_{B-L}} = \frac{c_B}{3} \frac{T_{\text{sph}}^2 m_\chi}{Y_B}, \quad (43)$$

where we note that $\dot{\Theta}(T_{\text{trap}}) \simeq m_\chi$ holds. For the scenario where $M_1^{\text{sym}}/z_{\text{in}} > T_{\text{sph}}$, this results in

$$\begin{aligned} T_{\text{trap}} &= \left(\frac{c_B}{3} Y_B^{-1} \left(\frac{2\pi^2}{45} g_* \right)^{-1} m_\chi T_{\text{sph}}^2 \right)^{1/3} \\ &\simeq 10^2 \text{ GeV} \left(\frac{m_\chi}{\text{keV}} \right)^{1/3}, \end{aligned} \quad (44)$$

where on the second line we have taken $Y_B = Y_B^{\text{osb}} \simeq 8.7 \times 10^{-11}$ [62]. For successful leptogenesis, it is imperative that $T_{\text{trap}} < T_{\text{sph}}$. Otherwise, the majoron rotation stops, and we lose the source of the CP phase during the leptogenesis. This means that we need the sufficiently light majoron, $m_\chi \leq \text{keV}$. On the other hand, $T_{\chi,\text{osc}}$ is given by

$$T_{\chi,\text{osc}} = 5 \times 10^5 \text{ GeV} \left(\frac{m_\chi}{\text{keV}} \right)^{1/2}, \quad (45)$$

which is much higher than T_{trap} at the mass range of m_χ that we are interested in. Therefore dark matter density in our model is evaluated in the manner of kinetic misalignment

¹⁰The potential overabundance due to the thermal production of majorons via $HL \leftrightarrow \chi N$ in thermal equilibrium, as discussed in [51], is negligible in our model. This is attributed to the sufficiently suppressed coupling constants between the majoron and right-handed neutrino, as outlined in Eq. (10).

mechanism, in which we have less redshift until now:

$$\frac{\rho_\chi}{s} \simeq \frac{m_\chi^2 f^2}{s(T_{\text{trap}})}, \quad (46)$$

where ρ_χ is energy density of majoron oscillation. In the case of $M_1^{\text{sym}}/z_{\text{in}} > T_{\text{sph}}$, the majoron abundance becomes

$$\frac{\Omega_\chi h^2}{\Omega_{\text{DM}} h^2} \simeq \left(\frac{m_\chi}{0.05 \text{ meV}} \right) \left(\frac{f}{6 \times 10^8 \text{ GeV}} \right)^2, \quad (47)$$

with $\Omega_{\text{DM}} h^2 \simeq 0.12$ is observed dark matter abundance [62].¹¹

In our model, the produced majoron can only decay to the neutrino pairs. The decay width of this majoron dark matter Γ_χ is given by

$$\Gamma_\chi \simeq \frac{1}{16\pi} \frac{m_\chi}{f^2} \sum_{i=1,2,3} m_i^2. \quad (48)$$

We note that the sum of neutrino mass squared can be predicted in our model, given as $\sum_i m_i^2 \simeq 0.005 \text{ eV}^2$ from neutrino oscillation data in the NuFit 5.2 analysis [57, 58] (without SK data). The lifetime of this majoron dark matter, denoted as τ_χ and equal to Γ_χ^{-1} , is tightly restricted from CMB and BAO analysis [87–91], and the lower limit is $\tau_\chi > 250 \text{ Gyr}$. This yields the following constraint to account for the dark matter abundance:

$$f \gtrsim 2 \times 10^6 \text{ GeV}, \quad m_\chi \lesssim 4 \text{ eV}. \quad (49)$$

Finally, By substituting Eq. (47) into Eqs. (41) and (42), we can show the parameter space where both the correct baryon asymmetry and dark matter density are achieved. For the $n = 5$, the expression for the baryon asymmetry is given by

$$\begin{aligned} Y_B &= \frac{1}{6} c_B Y_{B-L} \left(\frac{T_{\text{sph}}}{f} \right)^2 \\ &\simeq 9 \times 10^{-11} \left(\frac{\delta_{\text{eff}}}{1} \right) \left(\frac{T_{\text{sph}}}{130 \text{ GeV}} \right)^6 \left(\frac{S_i}{M_{\text{pl}}} \right)^{7/2} \\ &\quad \times \left(\frac{M_{\text{pl}}}{2.4 \times 10^{18} \text{ GeV}} \right) \left(\frac{10^{-2} \text{ GeV}}{m_S} \right)^{5/2} \left(\frac{10^7 \text{ GeV}}{f} \right)^{13/2}, \end{aligned} \quad (50)$$

and for the $n = 6$,

$$\begin{aligned} Y_B &= \frac{1}{6} c_B Y_{B-L} \left(\frac{T_{\text{sph}}}{f} \right)^2 \\ &\simeq 9 \times 10^{-11} \left(\frac{\delta_{\text{eff}}}{1} \right) \left(\frac{T_{\text{sph}}}{130 \text{ GeV}} \right)^6 \left(\frac{S_i}{M_{\text{pl}}} \right)^{7/2} \\ &\quad \times \left(\frac{M_{\text{pl}}}{2.4 \times 10^{18} \text{ GeV}} \right)^2 \left(\frac{2 \times 10^{-2} \text{ GeV}}{m_S} \right)^{5/2} \left(\frac{3 \times 10^8 \text{ GeV}}{f} \right)^{15/2}, \end{aligned} \quad (51)$$

¹¹In the case of $M_1^{\text{sym}}/z_{\text{in}} < T_{\text{sph}}$, we need large $\dot{\Theta}$ to generate the correct baryon asymmetry. This leads to the lower T_{trap} and larger majoron abundance.

where the parameters are fixed to satisfy Eq. (47). In each case, the expression for ϵ can be obtained by substituting m_χ , which can account for dark matter, and m_S , which can explain the BAU, into Eq. (25):

$$\epsilon \simeq \begin{cases} 4 \times 10^{-5} \delta_{\text{eff}}^{1/5} (f/\text{GeV})^{1/5}, & n = 5 \\ 0.2 \delta_{\text{eff}}^{1/5}, & n = 6 \end{cases} \quad (52)$$

thereby fulfilling the upper limit of ϵ , as given in Eq. (28).

4 Results

In this section, we discuss the prediction and allowed region in our model. Our analysis utilizes neutrino oscillation data from the NuFit 5.2 analysis [57, 58] (without SK data) as input parameters. To avoid constraints on the sum of light neutrino masses, $\sum_i m_i < (0.12 - 0.69)$ eV [59, 60], we set θ_{23} to the $+3\sigma$ range, consistent with Ref. [22]. This choice predicts a sum of the light neutrino masses $\sum_i m_i = 0.117$ eV and the PMNS phases $\delta \simeq 228^\circ$, $\alpha_2 = 225^\circ$, and $\alpha_3 = 70^\circ$ [22]. In addition to these, we introduce three free input parameters: λ , θ , and ϕ . In essence, λ determines the typical mass scale of right-handed neutrino masses, as expressed in Eq. (33). We concentrate on scenarios with a low $U(1)_{L_\mu-L_\tau}$ breaking scale, where $U(1)_{L_\mu-L_\tau}$ is restored in the early universe. This occurs when $\lambda \lesssim 8 \times 10^{-7}$, particularly within the central region of the $\phi - \theta$ plane. To account for the muon $g - 2$ anomaly, we require $\langle \sigma \rangle = 10 - 50$ GeV, necessitating a lower scale for λ , $\lambda \lesssim 5 \times 10^{-7}$ within the central region of the $\phi - \theta$ plane.

We examine two benchmark points: i) $\lambda = 8 \times 10^{-7}$, $\theta = 56^\circ$, and $\phi = 38^\circ$, resulting in $\lambda_{e\mu} \langle \sigma_\mu \rangle \simeq \lambda_{e\tau} \langle \sigma_\tau \rangle \simeq 123$ GeV, and the masses of right-handed neutrinos given by $M_1^{\text{sym}} \simeq 111$ GeV, $M_2^{\text{sym}} = M_3^{\text{sym}} \simeq 115$ GeV; ii) $\lambda = 4 \times 10^{-7}$, $\theta = 56^\circ$, and $\phi = 38^\circ$, yielding $\lambda_{e\mu} \langle \sigma_\mu \rangle \simeq \lambda_{e\tau} \langle \sigma_\tau \rangle \simeq 30$ GeV, aligning with the $U(1)_{L_\mu-L_\tau}$ breaking scale preferred by the muon $g - 2$ anomaly. At this point, we have $M_1^{\text{sym}} \simeq 28$ GeV, and $M_2^{\text{sym}} = M_3^{\text{sym}} \simeq 29$ GeV. In both cases, the $U(1)_{L_\mu-L_\tau}$ breaking scale is lower than the temperature where the sphaleron process decouples ($\langle \sigma \rangle < T_{\text{sph}}$), indicating leptogenesis occurs in the $U(1)_{L_\mu-L_\tau}$ symmetric phase. Also, we have verified that $M_1^{\text{sym}}/z_{\text{in}} > T_{\text{sph}}$ holds true for both benchmark points. Consequently, we do not encounter an additional suppression factor for the produced baryon asymmetry arising from the freeze-in mechanism.

We present our results in Figs. 3 and 4. In Fig. 3, the red and red dotted lines represent the parameter space where both the correct baryon asymmetry and dark matter density are achieved for $n = 5$ and $n = 6$, respectively, with $\delta_{\text{eff}} = 1$ in our model. In the light purple region, $H_{\text{osc}} := H(T_{\text{osc}})$ surpasses H_{inf} , undermining the justification for the large initial field value of Φ . The blue region is excluded based on the aforementioned CMB and BAO analyses [87–91], which set constraints on the lifetime of the majoron dark matter: $\tau_\chi < 250$ Gyr.

In Fig. 4, the blue line depicts the region where the correct dark matter abundance is achieved. Within the cyan region, the rotation of the majoron halts during leptogenesis, rendering our estimation unreliable. The blue region is again excluded based on the aforementioned CMB and BAO analyses [87–91], which constrain the majoron dark matter lifetime to $\tau_\chi < 250$ Gyr. The green region indicates that the $U(1)_{B-L}$ breaking field might be trapped in an undesirable minimum, preventing its rotation. This dependency

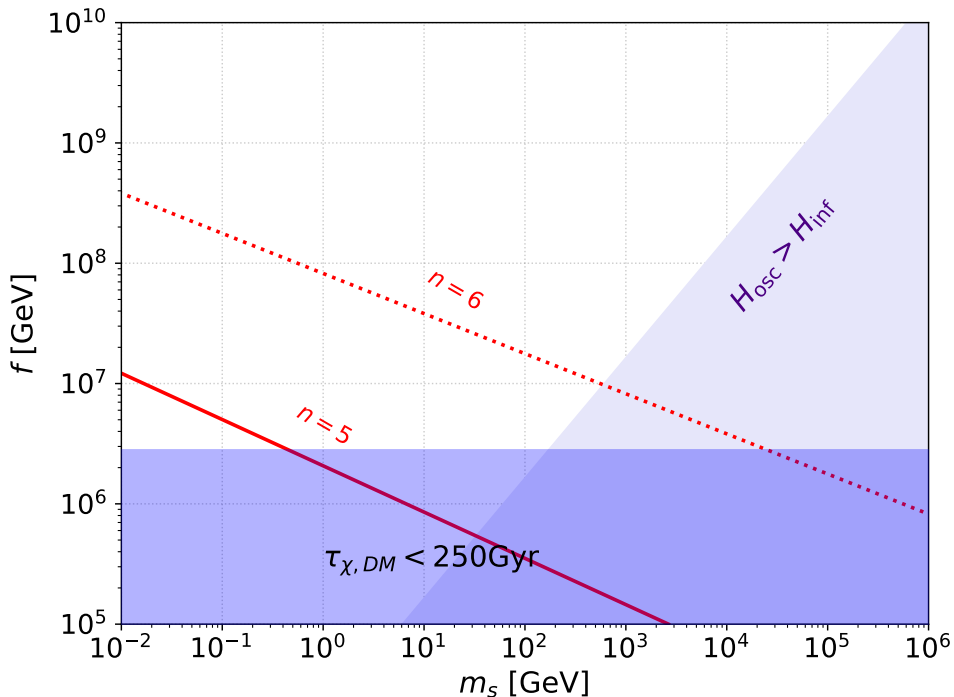


Figure 3: The parameter space where both the correct baryon asymmetry and dark matter abundance are achieved is depicted. The red and red dotted line represent the regions where the correct baryon asymmetry is obtained for $n = 5$ and $n = 6$ with $\delta_{\text{eff}} = 1$. In the light purple region, the value of $H_{\text{osc}} := H(T_{\text{osc}})$ surpasses H_{inf} thereby not justifying the large initial field value of Φ . The blue region is excluded based on constraints from CMB and BAO analyses [87–91], which limit the lifetime of the majoron dark matter to $\tau_\chi < 250$ Gyr.

is influenced by the magnitude of the effect of the higher-dimensional operator. For instance, we illustrate the case for $n = 5$ and $n = 6$ in Equation (17), assuming $\kappa \simeq 10^{-5}$, as suggested by the upper limit of κ in Eq.(16).

5 Summary and Discussions

In this work, we have considered the possibility of realizing the leptogenesis in $U(1)_{L_\mu-L_\tau}$ symmetric phase. It has been thought that it is hard to realize successful leptogenesis in the $U(1)_{L_\mu-L_\tau}$ symmetric phase, due to the lack of CP phase in the neutrino mass matrix caused by restriction from the gauge symmetry. However, our investigation reveals a promising avenue for successful leptogenesis by introducing an additional global $U(1)_{B-L}$ symmetry and a scalar field, denoted as Φ , responsible for breaking this symmetry. In the early universe, the rotation of Φ induces an additional chemical potential in the Boltzmann equation, facilitating successful leptogenesis. In our model, the higher-dimensional term breaking the global $U(1)_{B-L}$ symmetry gives a kick to the phase direction of the scalar Φ and leads to its rotation in the early universe. This mechanism is called the kinetic misalignment mechanism. Subsequently, as the Hubble friction causes a gradual decrease in the angular component’s kinetic energy, rotation halts when the majoron field

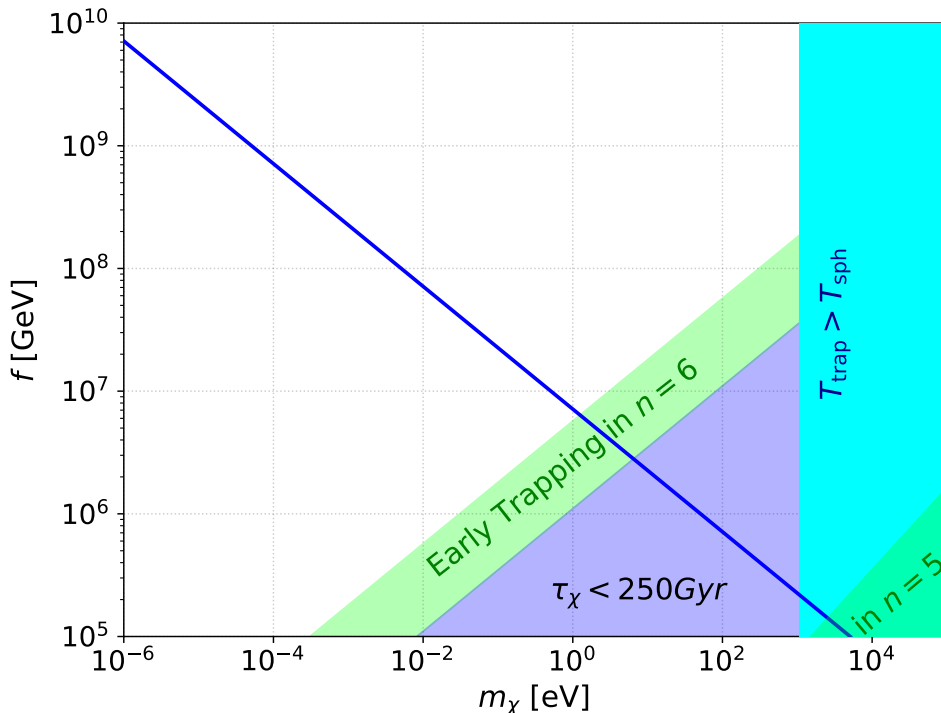


Figure 4: The parameter space that yields the correct dark matter abundance is depicted. The blue line represents the region where the correct dark matter density is achieved. Within the cyan region, the rotation of the majoron halts during leptogenesis, rendering our estimation unreliable. The green region suggests that the $U(1)_{B-L}$ breaking field might become trapped in an undesirable minimum, inhibiting its rotation. This behavior is influenced by the magnitude of the effect of the higher-dimensional operator, which gives the majoron mass. Here, we focus on $n = 5$ and $n = 6$ and show the case of $\kappa \simeq 10^{-5}$ as suggested by the upper limit of κ in Eq. (16). The blue region is excluded based on constraints from CMB and BAO analyses [87–91], which limit the lifetime of the majoron dark matter to $\tau_\chi < 250$ Gyr.

fails to overcome the potential barrier induced by the higher-dimensional operator term. Following this, the dark matter abundance is generated through the coherent oscillation of the majoron.

We have presented a model capable of predicting neutrino oscillation parameters by leveraging the presence of two zero minors in the mass matrix at low temperatures. This model introduces only three free parameters, namely λ , θ , and ϕ , which govern each component of the Majorana mass matrix and determine the characteristic scale of $U(1)_{L_\mu-L_\tau}$. Through a detailed analysis of these parameters, we observed that for $\lambda \lesssim 8 \times 10^{-7}$, the universe typically resides in the $U(1)_{L_\mu-L_\tau}$ symmetric phase. To assess the baryon asymmetry, we considered a quartic potential and higher dimensional operator for Φ and identified regions where both the correct baryon asymmetry and dark matter abundance can be generated. Importantly, this mechanism is expected to be applicable in a broader context, including models with more scalars breaking the gauged $U(1)_{L_\mu-L_\tau}$ symmetry. This generality arises from the unique determination of the Dirac and Majorana neutrino mass structures in the $U(1)_{L_\mu-L_\tau}$ symmetric phase, particularly in the context of the

type-I seesaw mechanism.

The adoption of a low-scale $U(1)_{L_\mu-L_\tau}$ symmetry finds motivation in various contexts. As an illustrative example, we focused on a benchmark scenario capable of explaining the muon $g - 2$ anomaly through loop corrections involving the $U(1)_{L_\mu-L_\tau}$ gauge boson Z' . Our proposed scenario is particularly effective in the context of leptogenesis when incorporating such a low-scale $U(1)_{L_\mu-L_\tau}$ symmetry.

Acknowledgements

We thank Koichi Hamaguchi and Natsumi Nagata for their helpful comments. This work is supported by JSPS KAKENHI Grant (22KJ1050).

A Derivation of Boltzmann equation in the kinetic motion of majoron background

In this appendix, we briefly illustrate the deviation of the Boltzmann equation Eq. (36) from the main text. Firstly, we explain how energy level splitting is realized due to the kinetic motion of the majoron background, leading to modified dispersion relations in the case of Dirac and Majorana fermions, as discussed in Refs. [45, 51]. Then, we demonstrate the deviation between the thermally averaged interaction rate and the inverse interaction rate in the presence of the kinetic majoron background. Finally, we derive the Boltzmann equation.

A.1 Energy level splitting

The kinetic motion of the majoron background $\dot{\Theta}$ modifies the equations of motion for Dirac and Majorana fermions, resulting in adjusted dispersion relations [45, 51]. This is because through this redefinition, we can eliminate the majoron field (or Θ dependence) in the original Lagrangian, leaving only the new interaction, which is derivative coupling with the majoron: $-\partial_\mu \Theta J_{B-L}^\mu/2$, where J_{B-L}^μ is the $B - L$ current, as explained in the main text.

In the case of Dirac fermion ψ_D , the Dirac equation becomes [45]:

$$(i\cancel{\partial} - m - \mu_\chi \gamma^0) \psi_D = 0, \quad (53)$$

where $\mu_\chi := \frac{1}{2}(B - L)_\psi \dot{\Theta}$. For ψ_D with momentum $p = (E_D, \mathbf{p})$, the dispersion relation changes to [45]:

$$E_{D\pm} = \sqrt{|\mathbf{p}|^2 + m^2} \mp \mu_\chi, \quad (54)$$

due to the non-zero contribution of μ_χ , contrary to $E_D = \sqrt{|\mathbf{p}|^2 + m^2}$ for $\mu_\chi = 0$, where the $+$ sign denotes the particle and the $-$ sign denotes the antiparticle. Thus, the term proportional to μ_χ causes energy level splittings between leptons and anti-leptons. This fact is crucial when considering the solution of the Dirac equation given by Eq. (53).

Assuming the time-dependence of μ_χ is negligible, i.e., $\ddot{\Theta} \simeq 0$, we can expand ψ_D into plane-wave solutions of the Dirac equation as follows[45]:

$$\psi_D(x) = \psi_{D,+}(x) + \psi_{D,-}(x), \quad (55)$$

$$\psi_{D,+}(x) = \sum_s \int \frac{d^3p}{(2\pi)^3} b_{\mathbf{p},s} u_{\mathbf{p},s} e^{-i\tilde{p}_{D,+}x}, \quad \psi_{D,-}(x) = \sum_s \int \frac{d^3p}{(2\pi)^3} d_{\mathbf{p},s}^\dagger v_{\mathbf{p},s} e^{i\tilde{p}_{D,-}x}, \quad (56)$$

where $\tilde{p}_{D,+} := (E_{D+}, \mathbf{p})$ and $\tilde{p}_{D,-} := (E_{D-}, \mathbf{p})$. The independent solutions $u_{\mathbf{p},s}$ and $v_{\mathbf{p},s}$ satisfy the Dirac equation for a particle and antiparticle, respectively, and hence, $b_{\mathbf{p},s}$ and $d_{\mathbf{p},s}$ are the creation and annihilation operators of particles and antiparticles. It should be noted that $u_{\mathbf{p},s}$ and $v_{\mathbf{p},s}$ are solutions defined for $\mu_\chi = 0$.

In the case of a Majorana fermion ψ_M , the equation of motion becomes [51]

$$(i\bar{\sigma}^\mu \partial_\mu - \mu_\chi) \psi_M = M\psi_M^\dagger, \quad (57)$$

where M represents the Majorana mass of ψ_M and we adopt a two-component spinor notation here. This equation leads to

$$(-\partial^2 - \mu_\chi^2 + 2i\mu_\chi \sigma^j \partial_j) \psi_M = M^2 \psi_M, \quad (58)$$

indicating energy level splittings between positive helicity and negative helicity states, denoted as $\psi_{M,\pm}$. For $\psi_{M,\pm}$ with momentum $p = (E_{M\pm}, \mathbf{p})$, the dispersion relation of $\psi_{M\pm}$ is given by [51]

$$\begin{aligned} E_{M\pm} &= \sqrt{|\mathbf{p}|^2 + M^2 + \mu_\chi^2 \mp 2\mu_\chi |\mathbf{p}|} \\ &\simeq \sqrt{|\mathbf{p}|^2 + M^2} \mp \mu_\chi v(\mathbf{p}), \end{aligned} \quad (59)$$

where $v(\mathbf{p}) = |\mathbf{p}|/\sqrt{|\mathbf{p}|^2 + M^2}$. Due to the non-zero contribution of μ_χ , we observe a different dispersion relation, contrary to $E_M = \sqrt{M^2 + |\mathbf{p}|^2}$ for $\mu_\chi = 0$. Assuming that the time-dependence of μ_χ is negligible, we can expand ψ_M into plane-wave solutions of the equation of motion as follows:

$$\psi_M(x) = \psi_{M,+}(x) + \psi_{M,-}(x), \quad (60)$$

$$\psi_{M,+}(x) = \int \frac{d^3p}{(2\pi)^3} a_{\mathbf{p},+} x_{\mathbf{p},+} e^{-i\tilde{p}_{M,+}x} + a_{\mathbf{p},+}^\dagger y_{\mathbf{p},+} e^{i\tilde{p}_{M,+}x} \quad (61)$$

$$\psi_{M,-}(x) = \int \frac{d^3p}{(2\pi)^3} a_{\mathbf{p},-} x_{\mathbf{p},-} e^{-i\tilde{p}_{M,-}x} + a_{\mathbf{p},-}^\dagger y_{\mathbf{p},-} e^{i\tilde{p}_{M,-}x}, \quad (62)$$

where $\tilde{p}_{M,+} := (E_{M+}, \mathbf{p})$ and $\tilde{p}_{M,-} := (E_{M-}, \mathbf{p})$. Here, $x_{\mathbf{p},s}$ and $y_{\mathbf{p},s}$ satisfy Dirac equations defined for $\mu_\chi = 0$, and $a_{\mathbf{p},s}$ and $a_{\mathbf{p},s}^\dagger$ are the creation and annihilation operators of this Majorana particle.

It is crucial to note that the dependence of μ_χ only appears in the exponential part of the plane wave, but not in the plane wave solutions that expand fermion fields, i.e., $u_{\mathbf{p},s}$, $v_{\mathbf{p},s}$, $x_{\mathbf{p},s}$, and $y_{\mathbf{p},s}$. This implies that the amplitude, \mathcal{M} , does not depend on μ_χ , and therefore, the \mathcal{S} matrix depends on μ_χ only through the δ -function of the four-momentum. This consideration is crucial for the subsequent computation.

A.2 Deviation between thermal-averaged interaction rate and inverse interaction rate

Next, let us compute the thermal-averaged decay rate and inverse decay rate. Importantly, due to the kinetic motion of the majoron background $\dot{\Theta}$, we observe a difference between the thermal-averaged decay rate and the inverse decay rate. It is noteworthy that the dynamic level splitting discussed in the previous subsection violates CPT-invariance.

First, let's focus on the interaction rate of the right-handed neutrino decaying into the lepton and Higgs, $N_i \rightarrow l_\alpha H$, and its inverse decay, $l_\alpha H \rightarrow N_i$. We assume that leptogenesis occurs in the $U(1)_{L_\mu - L_\tau}$ symmetric phase; hence, there is no CP phase in the amplitude \mathcal{M} . However, due to the dynamic level splitting, there is a dependence on $p_\chi := (\mu_\chi, \mathbf{0})$ in the δ -function of the four-momentum. Therefore, in the presence of the kinetic motion of the majoron background, the thermal-averaged interaction rate of $N_i \rightarrow l_\alpha H$ is given by

$$\langle \Gamma_{N_i \rightarrow l_\alpha H}^{\text{sym}, \Theta} \rangle = \frac{1}{n_{N_i}^{\text{eq}}} \int \frac{d^3 p_{N_i}}{(2\pi)^3 2E_{N_i}} 2M_1 f_{N_i}^{\text{eq}} \sum_{\pm} \Gamma_{N_{1,\pm} \rightarrow l_\alpha H}^{\text{sym}, \Theta}, \quad (63)$$

$$\Gamma_{N_{1,\pm} \rightarrow l_\alpha H}^{\text{sym}, \Theta} := \frac{1}{2M_1} \int \frac{d^3 p_H}{(2\pi)^3 2E_H} \int \frac{d^3 p_{l_\alpha}}{(2\pi)^3 2E_{l_\alpha}} \delta^4(\tilde{p}_{N_{1,\pm}} - \tilde{p}_{l_\alpha} - p_H) |\mathcal{M}(N_{1,\pm} \rightarrow l_\alpha H)|^2 \quad (64)$$

where $\tilde{p}_{N_{i,\pm}} := p_{N_i} \mp p_\chi v$, $\tilde{p}_{l_\alpha} := p_{l_\alpha} + p_\chi$, and we approximate the distribution functions by the Maxwell-Boltzmann distribution, $f_{N_i}^{\text{eq}} \simeq e^{-E_{N_i}/T}$. Similarly, the thermal-averaged interaction rate of $l_\alpha H \rightarrow N_i$ can be obtained as

$$\langle \Gamma_{l_\alpha H \rightarrow N_i}^{\text{sym}, \Theta} \rangle = \frac{1}{n_{N_i}^{\text{eq}}} \int \frac{d^3 p_{N_i}}{(2\pi)^3 2E_{N_i}} 2M_1 f_{N_i}^{\text{eq}} e^{-\mu_\chi/T} \sum_{\pm} e^{\mp \mu_\chi v/T} \Gamma_{N_{1,\pm} \rightarrow l_\alpha H}^{\text{sym}, \Theta}, \quad (65)$$

where we have approximated the distribution functions by the Maxwell-Boltzmann distribution, $f_{l_\alpha}^{\text{eq}} \simeq e^{-E_{l_\alpha}/T}$, $f_H^{\text{eq}} \simeq e^{-E_H/T}$, to derive this expression.

Up to the $O(\mu_\chi)$ order, this reduces to¹²

$$\langle \Gamma_{l_\alpha H \rightarrow N_i}^{\text{sym}, \Theta} \rangle \simeq \langle \Gamma_{N_i \rightarrow l_\alpha H}^{\text{sym}, \Theta} \rangle - \frac{\mu_\chi}{T} \langle \Gamma_{N_i \rightarrow l_\alpha H}^{\text{sym}} \rangle. \quad (67)$$

where $\langle \Gamma_{N_i \rightarrow l_\alpha H}^{\text{sym}} \rangle$ is the thermal-averaged interaction rate of $N_i \rightarrow l_\alpha H$ in the absence of the kinetic motion of the majoron background, given in Eq.(35).

Similarly, we can see that

$$\langle \Gamma_{\bar{l}_\alpha \bar{H} \rightarrow N_i}^{\text{sym}, \Theta} \rangle \simeq \langle \Gamma_{N_i \rightarrow \bar{l}_\alpha \bar{H}}^{\text{sym}, \Theta} \rangle + \frac{\mu_\chi}{T} \langle \Gamma_{N_i \rightarrow \bar{l}_\alpha \bar{H}}^{\text{sym}} \rangle. \quad (68)$$

¹²The interaction rate of decay for positive and negative helicity is the same in the absence of kinetic motion of the majoron background, $\Gamma_{N_{1,+} \rightarrow l_\alpha H}^{\text{sym}} = \Gamma_{N_{1,-} \rightarrow l_\alpha H}^{\text{sym}}$. Therefore, the μ_χ dependence from the dynamic level splitting of the right-handed neutrino is canceled out when we sum over the helicity states, up to $O(\mu_\chi)$:

$$\sum_{\pm} e^{\mp \mu_\chi v/T} \Gamma_{N_{1,\pm} \rightarrow l_\alpha H}^{\text{sym}, \Theta} = \sum_{\pm} \Gamma_{N_{1,\pm} \rightarrow l_\alpha H}^{\text{sym}, \Theta} + O(\mu_\chi^2). \quad (66)$$

We note that $\Gamma_{N_{1,\pm} \rightarrow l_\alpha H}^{\text{sym}, \Theta} = \Gamma_{N_{1,\pm} \rightarrow l_\alpha H}^{\text{sym}} + O(\mu_\chi)$.

Therefore, while the thermal-averaged interaction rate without $\dot{\Theta}$ background follows $\langle \Gamma_{l_\alpha H \rightarrow N_i}^{\text{sym}} \rangle = \langle \Gamma_{N_i \rightarrow l_\alpha H}^{\text{sym}} \rangle$, we have deviation between the thermal-averaged interaction rate and the inverse interaction rate due to the kinetic motion of the majoron background, which induces the non-zero chemical potential for the lepton (and Higgs), as we will explain below.

A.3 Derivation of the Boltzmann Equation

Now, we are ready to derive the Boltzmann equation for the lepton asymmetry in the presence of the kinetic motion of the majoron background. We approximate that the distribution function of X is given by $f_X(p) \simeq (n_X/n_X^{\text{eq}})f_X^{\text{eq}}(p)$, assuming kinetic equilibrium.

Furthermore, we approximate $f_X^{\text{eq}}(p)$ by Maxwell-Boltzmann distributions for $X = N, l_\alpha$, and H for simplicity. Then, the Boltzmann equations for the leptons and anti-leptons are as follows:¹³

$$\begin{aligned} \dot{n}_\alpha + 3Hn_\alpha &= \sum_i n_{N_i}^{\text{eq}} \langle \Gamma_{N_i \rightarrow l_\alpha H}^{\text{sym}, \Theta} \rangle \\ &\quad - \frac{n_\alpha n_H}{n_{l_\alpha}^{\text{eq}} n_H^{\text{eq}}} \sum_i n_{N_i}^{\text{eq}} \langle \Gamma_{l_\alpha H \rightarrow N_i}^{\text{sym}, \Theta} \rangle, \end{aligned} \quad (70)$$

$$\begin{aligned} \dot{\bar{n}}_\alpha + 3H\bar{n}_\alpha &= \sum_i n_{N_i}^{\text{eq}} \langle \Gamma_{N_i \rightarrow \bar{l}_\alpha \bar{H}}^{\text{sym}, \Theta} \rangle \\ &\quad - \frac{\bar{n}_\alpha n_{\bar{H}}}{n_{\bar{l}_\alpha}^{\text{eq}} n_{\bar{H}}^{\text{eq}}} \sum_i n_{N_i}^{\text{eq}} \langle \Gamma_{\bar{l}_\alpha \bar{H} \rightarrow N_i}^{\text{sym}, \Theta} \rangle, \end{aligned} \quad (71)$$

where we have neglected the lepton number violating scattering term because they are a higher order of $\lambda \ll 1$, and decoupled during the leptogenesis.

Then, using the relations obtained in the previous subsection, Eqs. (67) and (68), the Boltzmann equation for the lepton asymmetry density becomes

$$\dot{n}_{\Delta l_\alpha} + 3Hn_{\Delta l_\alpha} = - \sum_i n_{N_i}^{\text{eq}} \langle \Gamma_{N_i \rightarrow l_\alpha H}^{\text{sym}} \rangle \left(\frac{n_{\Delta l_\alpha}}{n_{l_\alpha}^{\text{eq}}} + \frac{n_{\Delta H}}{n_H^{\text{eq}}} - 2\frac{\mu_\chi}{T} \right), \quad (\alpha = e, \mu, \tau), \quad (72)$$

where $\mu_\chi = \dot{\Theta}/2$.

References

- [1] M. Fukugita and T. Yanagida, *Baryogenesis Without Grand Unification*, *Phys. Lett. B* **174** (1986) 45–47.

¹³The number density of positive and negative helicity states of the right-handed neutrino, denoted as $n_{N_i, \pm}$, should satisfy $\Delta n_{N_i, \pm} := n_{N_i, +} - n_{N_i, -} = O(\mu_\chi)$, and $\sum_\pm n_{N_i, \pm} = n_{N_i}^{\text{eq}}$, which means that we can express them as $n_{N_i, \pm} \simeq n_{N_i}^{\text{eq}} \pm \Delta n_{N_i, \pm}/2$. It should be noted that during leptogenesis, right-handed neutrinos are in thermal equilibrium in our model, $n_{N_i} = n_{N_i}^{\text{eq}}$. Using this relation, up to the order of $O(\mu_\chi)$, we have

$$\sum_\pm n_{N_i, \pm} \Gamma_{N_i, \pm \rightarrow l_\alpha H}^{\text{sym}, \Theta} = n_{N_i}^{\text{eq}} \sum_\pm \Gamma_{N_i, \pm \rightarrow l_\alpha H}^{\text{sym}, \Theta} + O(\mu_\chi^2), \quad (69)$$

which we use to derive the Boltzmann equations Eqs.(70) and(71).

- [2] V. A. Kuzmin, V. A. Rubakov, and M. E. Shaposhnikov, *On the Anomalous Electroweak Baryon Number Nonconservation in the Early Universe*, [Phys. Lett. B](#) **155** (1985) 36.
- [3] A. D. Sakharov, *Violation of CP Invariance, C asymmetry, and baryon asymmetry of the universe*, [Pisma Zh. Eksp. Teor. Fiz.](#) **5** (1967) 32–35.
- [4] P. Minkowski, *$\mu \rightarrow e\gamma$ at a Rate of One Out of 10^9 Muon Decays?*, [Phys. Lett.](#) **B67** (1977) 421–428.
- [5] T. Yanagida, *HORIZONTAL SYMMETRY AND MASSES OF NEUTRINOS*, [Conf. Proc.](#) **C7902131** (1979) 95–99.
- [6] M. Gell-Mann, P. Ramond, and R. Slansky, *Complex Spinors and Unified Theories*, [Conf. Proc.](#) **C790927** (1979) 315–321 [[arXiv:1306.4669](#)].
- [7] R. N. Mohapatra and G. Senjanovic, *Neutrino Mass and Spontaneous Parity Violation*, [Phys. Rev. Lett.](#) **44** (1980) 912.
- [8] **Particle Data Group** Collaboration, *Review of Particle Physics*, [PTEP](#) **2022** (2022) 083C01.
- [9] R. Foot, *New Physics From Electric Charge Quantization?*, [Mod. Phys. Lett. A](#) **6** (1991) 527–530.
- [10] X. G. He, G. C. Joshi, H. Lew, and R. R. Volkas, *NEW Z-prime PHENOMENOLOGY*, [Physical Review D](#) **43** (1991) 22–24.
- [11] X.-G. He, G. C. Joshi, H. Lew, and R. R. Volkas, *Simplest Z-prime model*, [Phys. Rev. D](#) **44** (1991) 2118–2132.
- [12] R. Foot, X. G. He, H. Lew, and R. R. Volkas, *Model for a light Z-prime boson*, [Phys. Rev. D](#) **50** (1994) 4571–4580 [[hep-ph/9401250](#)].
- [13] G. C. Branco, W. Grimus, and L. Lavoura, *The Seesaw Mechanism in the Presence of a Conserved Lepton Number*, [Nuclear Physics B](#) **312** (1989) 492–508.
- [14] S. Choubey and W. Rodejohann, *A Flavor symmetry for quasi-degenerate neutrinos: $L(\mu) - L(\tau)$* , [The European Physical Journal C](#) **40** (2005) 259–268 [[hep-ph/0411190](#)].
- [15] T. Araki, J. Heeck, and J. Kubo, *Vanishing Minors in the Neutrino Mass Matrix from Abelian Gauge Symmetries*, [Journal of High Energy Physics](#) **07** (2012) 083 [[arXiv:1203.4951](#)].
- [16] J. Heeck. PhD thesis, Heidelberg U., 2014.
- [17] A. Crivellin, G. D’Ambrosio, and J. Heeck, *Addressing the LHC flavor anomalies with horizontal gauge symmetries*, [Physical Review D](#) **91** (2015) 075006 [[arXiv:1503.03477](#)].

- [18] K. Asai, K. Hamaguchi, and N. Nagata, *Predictions for the neutrino parameters in the minimal gauged $U(1)_{L_\mu-L_\tau}$ model*, *Eur. Phys. J.* **C77** (2017) 763 [[arXiv:1705.00419](#)].
- [19] K. Asai, K. Hamaguchi, N. Nagata, S.-Y. Tseng, and K. Tsumura, *Minimal Gauged $U(1)_{L_\alpha-L_\beta}$ Models Driven into a Corner*, *Phys. Rev.* **D99** (2019) 055029 [[arXiv:1811.07571](#)].
- [20] K. Asai, *Predictions for the neutrino parameters in the minimal model extended by linear combination of $U(1)_{L_e-L_\mu}$, $U(1)_{L_\mu-L_\tau}$ and $U(1)_{B-L}$ gauge symmetries*, *Eur. Phys. J.* **C80** (2020) 76 [[arXiv:1907.04042](#)].
- [21] K. Asai, K. Hamaguchi, N. Nagata, and S.-Y. Tseng, *Leptogenesis in the minimal gauged $U(1)_{L_\mu-L_\tau}$ model and the sign of the cosmological baryon asymmetry*, *Journal of Cosmology and Astroparticle Physics* **11** (2020) 013 [[arXiv:2005.01039](#)].
- [22] A. Granelli, K. Hamaguchi, N. Nagata, M. E. Ramirez-Quezada, and J. Wada, *Thermal leptogenesis in the minimal gauged $U(1)_{L_\mu-L_\tau}$ model*, *JHEP* **09** (2023) 079 [[arXiv:2305.18100](#)].
- [23] S. N. Gninenko and N. V. Krasnikov, *The Muon anomalous magnetic moment and a new light gauge boson*, *Phys. Lett. B* **513** (2001) 119 [[hep-ph/0102222](#)].
- [24] S. Baek, N. G. Deshpande, X. G. He, and P. Ko, *Muon anomalous $g-2$ and gauged $L(\mu) - L(\tau)$ models*, *Phys. Rev. D* **64** (2001) 055006 [[hep-ph/0104141](#)].
- [25] B. Murakami, *The Impact of lepton flavor violating Z -prime bosons on muon $g-2$ and other muon observables*, *Phys. Rev. D* **65** (2002) 055003 [[hep-ph/0110095](#)].
- [26] E. Ma, D. P. Roy, and S. Roy, *Gauged $L(\mu) - L(\tau)$ with large muon anomalous magnetic moment and the bimaximal mixing of neutrinos*, *Phys. Lett. B* **525** (2002) 101–106 [[hep-ph/0110146](#)].
- [27] E. Ma and D. P. Roy, *Anomalous neutrino interaction, muon $g-2$, and atomic parity nonconservation*, *Phys. Rev. D* **65** (2002) 075021 [[hep-ph/0111385](#)].
- [28] M. Escudero, D. Hooper, G. Krnjaic, and M. Pierre, *Cosmology with A Very Light $L_\mu - L_\tau$ Gauge Boson*, *JHEP* **03** (2019) 071 [[arXiv:1901.02010](#)].
- [29] T. Araki, *et al.*, *Resolving the Hubble tension in a $U(1)_{L_\mu-L_\tau}$ model with the Majoron*, *PTEP* **2021** (2021) 103B05 [[arXiv:2103.07167](#)].
- [30] K. Asai, T. Moroi, and A. Niki, *Leptophilic Gauge Bosons at ILC Beam Dump Experiment*, *Phys. Lett. B* **818** (2021) 136374 [[arXiv:2104.00888](#)].
- [31] T. Moroi and A. Niki, *Leptophilic gauge bosons at lepton beam dump experiments*, *JHEP* **05** (2023) 016 [[arXiv:2205.11766](#)].
- [32] S. Baek and P. Ko, *Phenomenology of $U(1)(L(\mu)-L(\tau))$ charged dark matter at PAMELA and colliders*, *JCAP* **10** (2009) 011 [[arXiv:0811.1646](#)].

- [33] W. Altmannshofer, S. Gori, S. Profumo, and F. S. Queiroz, *Explaining dark matter and B decay anomalies with an $L_\mu - L_\tau$ model*, *JHEP* **12** (2016) 106 [[arXiv:1609.04026](#)].
- [34] G. Arcadi, T. Hugle, and F. S. Queiroz, *The Dark $L_\mu - L_\tau$ Rises via Kinetic Mixing*, *Phys. Lett. B* **784** (2018) 151–158 [[arXiv:1803.05723](#)].
- [35] M. Bauer, S. Diefenbacher, T. Plehn, M. Russell, and D. A. Camargo, *Dark Matter in Anomaly-Free Gauge Extensions*, *SciPost Phys.* **5** (2018) 036 [[arXiv:1805.01904](#)].
- [36] N. Okada and O. Seto, *Inelastic extra $U(1)$ charged scalar dark matter*, *Phys. Rev. D* **101** (2020) 023522 [[arXiv:1908.09277](#)].
- [37] D. Borah, A. Dasgupta, and D. Mahanta, *TeV scale resonant leptogenesis with L_μ - L_τ gauge symmetry in light of the muon $g-2$* , *Phys. Rev. D* **104** (2021) 075006 [[arXiv:2106.14410](#)].
- [38] S. Eijima, M. Ibe, and K. Murai, *Muon $g - 2$ and non-thermal leptogenesis in $U(1)_{L_\mu-L_\tau}$ model*, *JHEP* **05** (2023) 010 [[arXiv:2303.09751](#)].
- [39] I. Affleck and M. Dine, *A New Mechanism for Baryogenesis*, *Nucl. Phys. B* **249** (1985) 361–380.
- [40] M. Dine, L. Randall, and S. D. Thomas, *Baryogenesis from flat directions of the supersymmetric standard model*, *Nucl. Phys. B* **458** (1996) 291–326 [[hep-ph/9507453](#)].
- [41] R. T. Co, L. J. Hall, and K. Harigaya, *Axion Kinetic Misalignment Mechanism*, *Phys. Rev. Lett.* **124** (2020) 251802 [[arXiv:1910.14152](#)].
- [42] C.-F. Chang and Y. Cui, *New Perspectives on Axion Misalignment Mechanism*, *Phys. Rev. D* **102** (2020) 015003 [[arXiv:1911.11885](#)].
- [43] R. T. Co and K. Harigaya, *Axiogenesis*, *Phys. Rev. Lett.* **124** (2020) 111602 [[arXiv:1910.02080](#)].
- [44] A. Kusenko, K. Schmitz, and T. T. Yanagida, *Leptogenesis via Axion Oscillations after Inflation*, *Phys. Rev. Lett.* **115** (2015) 011302 [[arXiv:1412.2043](#)].
- [45] M. Ibe and K. Kaneta, *Spontaneous thermal Leptogenesis via Majoron oscillation*, *Phys. Rev. D* **92** (2015) 035019 [[arXiv:1504.04125](#)].
- [46] V. Domcke, Y. Ema, K. Mukaida, and M. Yamada, *Spontaneous Baryogenesis from Axions with Generic Couplings*, *JHEP* **08** (2020) 096 [[arXiv:2006.03148](#)].
- [47] R. T. Co, N. Fernandez, A. Ghalsasi, L. J. Hall, and K. Harigaya, *Lepto-Axiogenesis*, *JHEP* **03** (2021) 017 [[arXiv:2006.05687](#)].
- [48] V. Domcke, K. Kamada, K. Mukaida, K. Schmitz, and M. Yamada, *Wash-In Leptogenesis*, *Phys. Rev. Lett.* **126** (2021) 201802 [[arXiv:2011.09347](#)].

- [49] M. Berbig, *Diraxiogenesis*, *JHEP* **01** (2024) 061 [[arXiv:2307.14121](#)].
- [50] W. Chao and Y.-Q. Peng, *Majorana Majoron and the Baryon Asymmetry of the Universe*, [arXiv:2311.06469](#) (2023).
- [51] E. J. Chun and T. H. Jung, *Leptogenesis driven by a Majoron*, *Phys. Rev. D* **109** (2024) 095004 [[arXiv:2311.09005](#)].
- [52] P. Barnes, R. T. Co, K. Harigaya, and A. Pierce, *Lepto-axiogenesis with light right-handed neutrinos*, [arXiv:2402.10263](#) (2024).
- [53] K. Harigaya, T. Igari, M. M. Nojiri, M. Takeuchi, and K. Tobe, *Muon $g-2$ and LHC phenomenology in the $L_\mu - L_\tau$ gauge symmetric model*, *JHEP* **03** (2014) 105 [[arXiv:1311.0870](#)].
- [54] Y. Kaneta and T. Shimomura, *On the possibility of a search for the $L_\mu - L_\tau$ gauge boson at Belle-II and neutrino beam experiments*, *PTEP* **2017** (2017) 053B04 [[arXiv:1701.00156](#)].
- [55] T. Nomura and T. Shimomura, *Searching for scalar boson decaying into light Z' boson at collider experiments in $U(1)_{L_\mu-L_\tau}$ model*, *Eur. Phys. J.* **C79** (2019) 594 [[arXiv:1803.00842](#)].
- [56] H. K. Dreiner, H. E. Haber, and S. P. Martin, *Two-component spinor techniques and Feynman rules for quantum field theory and supersymmetry*, *Physics Reports* **494** (2010) 1–196 [[arXiv:0812.1594](#)].
- [57] **NuFIT** Collaboration, *NuFIT v5.2*, <http://www.nu-fit.org>.
- [58] I. Esteban, M. C. Gonzalez-Garcia, M. Maltoni, T. Schwetz, and A. Zhou, *The fate of hints: updated global analysis of three-flavor neutrino oscillations*, *Journal of High Energy Physics* **09** (2020) 178 [[arXiv:2007.14792](#)].
- [59] J. Lesgourgues and L. Verde in P. A. Zyla et al. (Particle Data Group), *Neutrinos in Cosmology (Review of Particle Physics)*, *Progress of Theoretical and Experimental Physics* **2020** (2020) 083C01.
- [60] F. Capozzi, *et al.*, *Addendum to “Global constraints on absolute neutrino masses and their ordering”*, *Physical Review D* **101** (2020) 116013.
- [61] S. Vagnozzi, *et al.*, *Unveiling ν secrets with cosmological data: neutrino masses and mass hierarchy*, *Phys. Rev. D* **96** (2017) 123503 [[arXiv:1701.08172](#)].
- [62] **Planck** Collaboration, *Planck 2018 results. VI. Cosmological parameters*, *Astronomy & Astrophysics* **641** (2020) A6 [[arXiv:1807.06209](#)]. [Erratum: *Astron.Astrophys.* 652, C4 (2021)].
- [63] S. Roy Choudhury and S. Hannestad, *Updated results on neutrino mass and mass hierarchy from cosmology with Planck 2018 likelihoods*, *Journal of Cosmology and Astroparticle Physics* **07** (2020) 037 [[arXiv:1907.12598](#)].

- [64] M. M. Ivanov, M. Simonović, and M. Zaldarriaga, *Cosmological Parameters and Neutrino Masses from the Final Planck and Full-Shape BOSS Data*, *Physical Review D* **101** (2020) 083504 [[arXiv:1912.08208](#)].
- [65] **DES** Collaboration, *Dark Energy Survey Year 3 results: Cosmological constraints from galaxy clustering and weak lensing*, *Physical Review D* **105** (2022) 023520 [[arXiv:2105.13549](#)].
- [66] I. Tanseri, S. Hagstotz, S. Vagnozzi, E. Giusarma, and K. Freese, *Updated neutrino mass constraints from galaxy clustering and CMB lensing-galaxy cross-correlation measurements*, *JHEAp* **36** (2022) 1–26 [[arXiv:2207.01913](#)].
- [67] **NA64** Collaboration, *First Results in the Search for Dark Sectors at NA64 with the CERN SPS High Energy Muon Beam*, *Phys. Rev. Lett.* **132** (2024) 211803 [[arXiv:2401.01708](#)].
- [68] **BaBar** Collaboration, *Search for a muonic dark force at BABAR*, *Phys. Rev. D* **94** (2016) 011102 [[arXiv:1606.03501](#)].
- [69] **CMS** Collaboration, *Search for an $L_\mu - L_\tau$ gauge boson using $Z \rightarrow 4\mu$ events in proton-proton collisions at $\sqrt{s} = 13$ TeV*, *Phys. Lett. B* **792** (2019) 345–368 [[arXiv:1808.03684](#)].
- [70] G. Bellini *et al.*, *Precision measurement of the ${}^7\text{Be}$ solar neutrino interaction rate in Borexino*, *Phys. Rev. Lett.* **107** (2011) 141302 [[arXiv:1104.1816](#)].
- [71] **CHARM-II** Collaboration, *First observation of neutrino trident production*, *Phys. Lett. B* **245** (1990) 271–275.
- [72] **CCFR** Collaboration, *Neutrino tridents and $W Z$ interference*, *Phys. Rev. Lett.* **66** (1991) 3117–3120.
- [73] M. Dine, L. Randall, and S. D. Thomas, *Supersymmetry breaking in the early universe*, *Phys. Rev. Lett.* **75** (1995) 398–401 [[hep-ph/9503303](#)].
- [74] **Planck** Collaboration, *Planck 2018 results. X. Constraints on inflation*, *Astron. Astrophys.* **641** (2020) A10 [[arXiv:1807.06211](#)].
- [75] M. Kawasaki and K. Nakayama, *Affleck-Dine baryogenesis in anomaly-mediated SUSY breaking*, *JCAP* **02** (2007) 002 [[hep-ph/0611320](#)].
- [76] K. Enomoto, K. Hamaguchi, K. Kamada, and J. Wada, *Revisiting Affleck-Dine leptogenesis with light sleptons*, *JCAP* **07** (2023) 003 [[arXiv:2304.05614](#)].
- [77] R. Barbieri, P. Creminelli, A. Strumia, and N. Tetradis, *Baryogenesis through leptogenesis*, *Nucl. Phys. B* **575** (2000) 61–77 [[hep-ph/9911315](#)].
- [78] G. Engelhard, Y. Grossman, E. Nardi, and Y. Nir, *The Importance of N_2 leptogenesis*, *Phys. Rev. Lett.* **99** (2007) 081802 [[hep-ph/0612187](#)].
- [79] S. Antusch, P. Di Bari, D. A. Jones, and S. F. King, *A fuller flavour treatment of N_2 -dominated leptogenesis*, *Nucl. Phys. B* **856** (2012) 180–209 [[arXiv:1003.5132](#)].

- [80] S. Blanchet, P. Di Bari, D. A. Jones, and L. Marzola, *Leptogenesis with heavy neutrino flavours: from density matrix to Boltzmann equations*, *JCAP* **01** (2013) 041 [[arXiv:1112.4528](#)].
- [81] A. Abada, S. Davidson, F.-X. Josse-Michaux, M. Losada, and A. Riotto, *Flavor issues in leptogenesis*, *JCAP* **04** (2006) 004 [[hep-ph/0601083](#)].
- [82] E. Nardi, Y. Nir, E. Roulet, and J. Racker, *The Importance of flavor in leptogenesis*, *JHEP* **01** (2006) 164 [[hep-ph/0601084](#)].
- [83] W. Buchmuller, P. Di Bari, and M. Plumacher, *Leptogenesis for pedestrians*, *Annals Phys.* **315** (2005) 305–351 [[hep-ph/0401240](#)].
- [84] J. Preskill, M. B. Wise, and F. Wilczek, *Cosmology of the Invisible Axion*, *Phys. Lett. B* **120** (1983) 127–132.
- [85] L. F. Abbott and P. Sikivie, *A Cosmological Bound on the Invisible Axion*, *Phys. Lett. B* **120** (1983) 133–136.
- [86] M. Dine and W. Fischler, *The Not So Harmless Axion*, *Phys. Lett. B* **120** (1983) 137–141.
- [87] B. Audren, J. Lesgourgues, G. Mangano, P. D. Serpico, and T. Tram, *Strongest model-independent bound on the lifetime of Dark Matter*, *JCAP* **12** (2014) 028 [[arXiv:1407.2418](#)].
- [88] K. Enqvist, S. Nadathur, T. Sekiguchi, and T. Takahashi, *Constraints on decaying dark matter from weak lensing and cluster counts*, *JCAP* **04** (2020) 015 [[arXiv:1906.09112](#)].
- [89] A. Nygaard, T. Tram, and S. Hannestad, *Updated constraints on decaying cold dark matter*, *JCAP* **05** (2021) 017 [[arXiv:2011.01632](#)].
- [90] S. Alvi, T. Brinckmann, M. Gerbino, M. Lattanzi, and L. Pagano, *Do you smell something decaying? Updated linear constraints on decaying dark matter scenarios*, *JCAP* **11** (2022) 015 [[arXiv:2205.05636](#)].
- [91] T. Simon, G. Franco Abellán, P. Du, V. Poulin, and Y. Tsai, *Constraining decaying dark matter with BOSS data and the effective field theory of large-scale structures*, *Phys. Rev. D* **106** (2022) 023516 [[arXiv:2203.07440](#)].